

Sept. 26, 2014

To: David Sassani (SNL)

From: Peter C. Rieke

cc: Joe Ryan John Vienna (PNNL)

Approved by: _____

Name, Technical Reviewer Date

Approved by: _____

Name, Program Manager Date

Title: Letter Report on Completion of Milestone – “Preparation of a Beta Phase User Manual”

Milestone: M4FT-14PN0804044

Title Page

***Letter Report on Completion of Milestone –
“Preparation of a Beta Phase User Manual”
Milestone: M4FT-14PN0804044***

Prepared for

U.S. Department of Energy

Used Fuel Disposition Campaign

Peter C. Rieke, Joe Ryan

Pacific Northwest National Laboratory

Sept 26, 2014

FCRD-UFD-2014-000482



Pacific Northwest
NATIONAL LABORATORY

*Proudly Operated by **Battelle** Since 1965*

DISCLAIMER

This information was prepared as an account of work sponsored by an agency of the U.S. Government. Neither the U.S. Government nor any agency thereof, nor any of their employees, makes any warranty, expressed or implied, or assumes any legal liability or responsibility for the accuracy, completeness, or usefulness, of any information, apparatus, product, or process disclosed, or represents that its use would not infringe privately owned rights. References herein to any specific commercial product, process, or service by trade name, trade mark, manufacturer, or otherwise, does not necessarily constitute or imply its endorsement, recommendation, or favoring by the U.S. Government or any agency thereof. The views and opinions of authors expressed herein do not necessarily state or reflect those of the U.S. Government or any agency thereof.

Figures

Fig. 1 Influence of the parameter p from Eqn. 2 on the diffusion of free vacancies out of a purely unreactive silicate glass.10

Fig. 2 Formation of an erosion interface in a simple reactive silicate glass.11

Fig. 3 Elemental distributions at $t=1.0$ sec for Si, B, Na and H₂O.12

Fig. 4 Proposed chemical reaction model and fit of that model to TOF-SIMS glass corrosion data.15

Fig. 5 Layer thickness and solution concentration for $Q/V = 1e-8$ [1/s].15

Fig. 6 Plots obtained from example of optimizing the AH model against selected LAWA44 data.30

Fig.7 Example of output plot for optimization of Exp_12 data to the GRAAL model.33

Tables

Table 1. List of Chemical Reactions Considered in the Model. 9

Acronyms and Abbreviations

PNNL	Pacific Northwest National Laboratory
DOE	US Department of Energy
FCRD	Fuel Cycle Research & Development
GCMT	Glass Corrosion Modeling Tool
SPFT	Single Pass Flow Through
PCT	Product Consistency Test
PUF	Pressurized Unsaturated Flow
PEST	Parameter Estimation Software Package
AH	Aagaard-Helgeson
GM	Grambow-Muller
GRAAL	Glass Reactivity with Allowance for the Alteration Layer
SON68	Nonradioactive glass developed by French Alternative Energies and Atomic Energy Commission
LAW	Low Activity Waste
TOF-SIMS	Time of Flight, Secondary Ion Mass Spectroscopy
APT	Atom Probe Tomography
PDE	Partial Differential Equation
ALTGLASS	Glass corrosion database prepared by Savannah River National Laboratory
ICP	Inductively Coupled Plasma
PA	Performance Assessment
GUI	Graphical User Interface

Summary

This report describes the work performed to meet milestone M4FT-14PN0804044 “Preparation of a Beta Phase User Manual” for the FT-14PN0804043 – Comprehensive Corrosion Model Evaluation Tool – PNNL project.

The Glass Corrosion Modeling Tool or GCMT allows the user to evaluate the goodness of a glass alteration model by fitting the model to a selected experimental database. The GCMT can implement the models proposed by various workers in the glass chemistry community and adds new models or variations as they become available. Extensive databases of glass dissolution data can be accessed. The GCMT can be used to understand the strengths and weaknesses of a particular model and propose new or adapted models. Given a specific model, the GCMT can be used to validate the choice of parameters used in the model for the targeted application. The GCMT should be of value in choosing a glass dissolution source term for the Performance Assessment (PA) nuclear waste repository model.

The GCMT has seen significant advancement and has been utilized in new applications. A draft “User Manual” is in preparation for an upcoming milestone due in September 2014. The following improvements were made to the GCMT since the last milestone report in Sept of 2013:

- 1) The ALTGLASS database prepared by SRNL was integrated into the GCMT and a graphical user interface developed to allow easy selection of database subsets for specific analysis.
- 2) TOF-SIMS and APT depth profiling data as well as SPFT dissolution data, from PNNL isotope swap experiments, were converted to a form for import into the GCMT. Methods for quantitative interpretation of the depth profiling data were developed.
- 3) A new chemistry and physics base model of glass alteration was developed that allows prediction of depth profiling data. The PDEs describing diffusion and chemical reaction (DCRx model) are presented in sufficient depth for others to reproduce the model.
- 4) The DCRx model was tested against TOF-SIMS data using the GCMT and adaptations to the model were proposed.
- 5) The GCMT was used to qualitatively understand the impact of ion exchange on the dissolution of ILAW glasses using an adapted GRAAL model.
- 6) A new DCRx model was developed which accounts for formation of ionic species. Preliminary model behavior and results are reported.

Comprehensive Corrosion Model Evaluation Tool

Milestone Report M4FT-14PN0804044 “Preparation of a Beta Phase User Manual”

Peter C. Rieke, Joe Ryan,

Pacific Northwest National Laboratory, Richland, WA

Contents

Title Page.....	i
Figures.....	iii
Tables.....	iii
Acronyms and Abbreviations.....	iii
Summary.....	iv
Introduction.....	2
Developments and Additions to the GCMT Code.....	3
Development of a GUI for the ALTGLASS database.....	3
Addition of Depth Profile Databases.....	4
Formulation of a Model to Predict Depth Profile Data.....	4
Extension of the DCR Model to Include Ionic Species.....	6
Introduction.....	6
Model Transport.....	7
Source and Sink Terms – The Chemical Reaction Set.....	9
Selected Results.....	11
Discussion.....	14
Conclusions.....	15
Future Work.....	16
New Applications.....	16
Modeling Depth Profiling Data.....	16

Residual Rate Effects in ILAW Glasses.....	18
Appendix A. Preliminary User Manual.....	19
Introduction	19
Obtaining Using the GCMT.....	20
Overview of the Mechanisms of Glass Alteration.....	21
Description of Models.....	22
The Aagaard-Helgeson Model with Residual Rate [1-3]	22
The Grambow-Muller Model [4-9].....	23
The GRAAL Model [10-12].....	25
Diffusive Chemical Reaction (DCRx) Model	26
Commonality and Differences	28
Comparison of the DCRx and Reactive Transport.....	29
Databases available in the GCMT	30
Examples of GCMT Uses.....	31
Example1. Optimizing the AH model against LAWA44 SPFT data	31
Example2. Optimizing the GRAAL Model against Time Dependent SON68 Data.....	33
Example3. GUI for the ALTGLASS database	38
References	39

Introduction

The Glass Corrosion Modeling Tool or GCMT allows the user to evaluate the goodness of a glass alteration model by fitting the model to a selected experimental database. It returns the best estimate of the model parameters. The GCMT allows comparison of different models and ultimately allows a scientific method of choosing the best possible model. By this means researchers can understand how particular models succeed or fail in explaining certain results and allow them to modify the models on a rational basis. Engineers can use the tool to quantitatively justify the choice of a certain model of glass dissolution and the associated parameters values used in the model. Those models can then be used in codes used to predict the durability and lifetime of nuclear waste packages.

The GCMT consists of a set of software packages that interact to statistically optimize key parameters, such as rate constants or activation energies, in a glass alteration model to a selected set of experimental data. Glass alteration data imported into the GCMT may be of any type provided the model is capable of predicting those data. Four databases are current supplied with the tool. Currently the Aagaard-Helgeson (AH) [1-3] with residual rate, Grambow-Muller (GM) [4-

9] and Glass Reactivity with Allowance for the Alteration Layer (GRAAL) [10-12] models can be implemented. Two new models have been developed to predict depth profiling data provided by Time of Flight, Secondary Ion Mass Spectrometry (TOF-SIMS) and Atomic Probe Tomography (APT) studies. For a given choice of database and model, the GCMT repeatedly implements the model solver until the statistical fitting package determines the best estimate of the parameters has been found. The model solver may be a simple code of a few lines embedded in the GCMT or it may be an advanced computational fluid dynamics code interacting with a chemical kinetics and thermodynamics package. Complex geometries or experimental configuration may be modeled but in practice the available data do not warrant detailed studies.

This document summarizes both applications of and developments in the GCMT since the last major project report was submitted in Sept. of 2013. Also attached is a preliminary draft of a GCMT User's Manual. The manual can currently be used by knowledgeable users to implement the GCMT for their own applications.

Developments and Additions to the GCMT Code

Development of a GUI for the ALTGLASS database

A graphical user interface (GUI) was constructed for easy access to the very large ALTGLASS database put together by Carol Jantzen at Savannah River National Laboratory[13]. ALTGLASS contains a wealth of information for each experimental point including the glass oxide composition, the leachate concentrations, temperature, flow rate, pH etc. Some 68 values are reported for each for the nearly 2000 experiments. This makes it very difficult to parse through the database and find similar experiments or identify possible trends. In addition the ALTGLASS database could provide a useful input to the GCMT provided there was a convenient way to select desired data. Towards this end, a GUI for ALTGLASS was constructed using MatLab. The GUI allows any of the 68 values to be narrowed by either text value, e.g. sample ID, or by numerical value, e.g. leachate pH. After down selecting desired datasets, the values can be plotted for visual examination. The data sets can then be imported into the GCMT. Details for its use are covered in the GCMT User Manual.

The ALTGLASS database contains mostly SPFT tests taken at one or at most a few sampling times. Hence it lacks important information necessary to develop new chemistry and physics based models. However the database covers a very wide range of glass compositions and could allow rate constant to be expressed in terms of glass composition. The glass corrosion model to be used for the radionuclide source term in the Performance Assessment (PA) model is still under debate. The ALTGLASS database used in the GCMT would allow specification of a generalized yet reasonably simple glass corrosion model needed for the PA model [14-16].

Addition of Depth Profile Databases

Work at PNNL has resulted in an unprecedented picture of glass alteration using TOF-SIMS and APT experimental techniques to quantify the depth profiles of elements in leached SON68 glass [17]. Further an isotopic swap technique allowed ambiguities in the time evolution of the elemental distributions to be resolved. The leachate elemental concentrations were also determined using ICP allowing the results to be compared with other leaching data such as that in the ALTGLASS database. Our intent is to utilize the GCMT to quantitatively analyze this data. However, the datasets are very large, not particularly amenable to direct importation and the signal intensities don't directly represent the mole fraction quantities need in models. MatLab was used to import the experimental data files and select and organize the important numerical information.

More importantly each data set was also converted to a value representing the local elemental mole fraction. To date we have reduced the importation of the TOF-SIMS and APT data to a series of numerical steps that allow adjustment of the "calibration" process. This has been completed for the TOF-SIMS data and an example of the data is discussed below. The APT data sets have been collected and imported in the original numerical form and we are consulting with the analytical experts to convert the signal intensity data to mole fraction data. Generally speaking, the first steps are to account for instrumental artifacts and then to normalize the data to the known composition of the pristine glass.

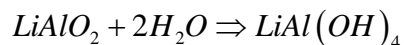
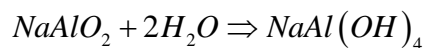
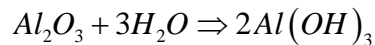
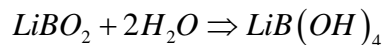
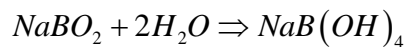
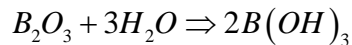
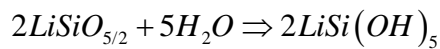
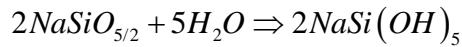
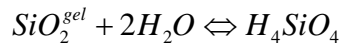
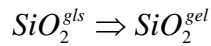
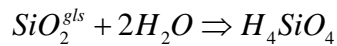
Finally the TOF-SIMS and APT data must be integrated with the ICP analysis of the leachate solutions. Each of these analytical techniques has a numerical uncertainty associated with the signal acquisition process as well as the data calibration process. This uncertainty will have to be converted to an appropriate weighting factor to be input into the PEST parameter optimization module in the GCMT.

Formulation of a Model to Predict Depth Profile Data

The new depth profiling data described above cannot be modeled using existing glass corrosion models. The AH, GM and GRAAL models all assume the formation of one or more interfaces to predict the mass of glass leached into solution. They cannot, however, predict how these apparent interfaces are formed from an otherwise continuous medium.

A new model was formulated and implemented in the GCMT to remedy this lack. The model is based upon an extensible set of chemical reactions with these reactions forming species with diffuse out of the glass into the leachate solution. Hence we refer to this model as the Diffusive Chemical Reaction (DCRx) model. Below we briefly review the assumptions behind the model.

The set of chemical reactions considered here are



The immobile species found in glass (as determined from NMR data, for example [18-24]) - on the left side of these stoichiometric equations- react with water, to form neutral or ion pair species. These species - on the right of the equations – are, along with water, assumed to be mobile. The model is extensible in that new secondary or intermediate reactions can be added as needed to explain experimental data. For example, this current version of the model clearly ignores the formation of ionic species but provides a set of reactions that encompass those chemical possibilities.

In addition, the diffusivity of various species is assumed to be impacted primarily by the local concentration of water with a minimal diffusivity as determined by solid state diffusion in the “dry” or pristine glass. This allows transport of most species, except water, to be described by simple Fickian diffusion. Tomozawa [25-29] and Zhang [30-34] have suggested from experimental data that the effective diffusivity of water in glass is proportional to the water content. Thus the diffusivity of each species may be described by a power dependence of diffusivity on water content such as

$$D_i = D_i^0 (X_{H_2O})^n + D_i^{gls}$$

Where X_{H_2O} is the local mole fraction of water and D_i^0 is the diffusivity in pure water. D_i^{gls} is the diffusivity in dry glass. There are other rational approaches to determine the diffusivity but this discussion is beyond the scope of this report and we believe this is an adequate approach until the set of relevant chemical reactions is more clearly defined.

Water in this model is unique in that it is assumed to 1) be the species diffusing into a region left vacant by any other diffusing species and 2) diffuses into dry glass using a free volume model. This significantly simplifies the transport and source terms in the partial differential equations (PDE) needed in the model.

These transport and source equations (the details of which have been omitted for brevity but can be obtained from the author) were implemented as a COMSOL file that can be initiated through MatLab. Selected TOF-SIMS data were then fit by optimizing the model parameters using the GCMT. More details of the results are discussed below.

The DCRx is a model of glass dissolution that specifies which fundamental physical transport equations are used, the approximations that may be made, the set of chemical reactions and species being considered and the dependence of diffusivity on local composition. It is often difficult or impossible to determine what equations are being used in other “continuum” models of glass alteration. As the DCRx is based upon a set of PDEs describing fundamental physics and chemistry, it is an extensible model. Any simplification can be relaxed or additional chemical reactions added as needed. This is in contrast to the AH, GM and GRAAL models which are phenomenological in that they may predict the correct dissolution rate of the glass, they do so by extending the equations beyond their applicability or impose non-physical assumptions on the rate of dissolution. This makes it difficult to modify them in light of new experimental evidence. The GRAAL model for example cannot predict TOF-SIMS or APT elemental distributions.

Extension of the DCR Model to Include Ionic Species

Introduction

TOF-SIMS and APT data accompanied by ICP analysis of dissolved species in solution provide a detailed picture of how various elements are leached from glass. [17] This extensive data is also complemented by isotopic swap experiments that provide even more detail about the rates at which various species diffuse into or out of the glass and undergo chemical reaction. These data provide only the elemental distributions and do not identify what particular species are being created within the glass and diffusing to the exterior solution.

These data support the basic presumptions about the mechanisms of glass dissolution that have been developed by the glass corrosion community. [9, 11, 35-39] These mechanisms are often described as the formation of various layers and associated interfaces that evolve in composition and thickness with time. These layers have been given various names but for our discussion we describe them as five regions. These are

- 1) The Erosion Layer -- A layer of some thickness in which the glass has completely dissolved and is replaced by water. The interface with the adjoining gel layer appears to be sharp once removed from solution but may in fact be somewhat diffuse while in contact with water.

- 2) The Gel Layer– A layer depleted of most soluble oxides (e.g. B₂O₃) and alkali cations (e.g. Na and Li). This layer may be partially depleted of Silicon and Aluminum. The extent of depletion of these residual species may vary with depth. The SiO₂ as found in pristine glass may undergo transition by dissolution/reprecipitation or rearrangement to a more stable silicate that has some characteristics of a stable chemical phase and resembles the gel material formed by sol-gel processes.
- 3) The Transition Layer– In this region borates and alkaline oxides are reacting with water to form species which diffuse through the gel layer into the contacting solution. Silicates, Aluminates and other species which can form anionic oxides in solution may partially hydrolyze but do not form mobile species.
- 4) The Ion Exchange Layer– Protons as bare H⁺ diffuse into the dry glass and exchange with Na⁺ or Li⁺. The extent of this process is of some debate but the apparent consensus is that ion exchange is necessary for subsequent diffusion of water into this region. Possibly the structure opens up or the formation of silanol groups provides a low energy site into which water can move.
- 5) The Pristine Glass– This semi-infinite layer is the as prepared glass whose composition is fairly well known from the oxide composition and NMR studies of the species formed in glass. In this work the SON68 glass is used to generate the pristine glass speciation as the TOF-SIMS and APT data were conducted on this material.

The objective of this model is to use fundamentally sound mass transport and chemical reaction scheme [40-42] to predict the formation of regions such as those described above. It is important to note that pristine glass is an amorphous material with no significant variation in composition or structure over dimensions greater than about 5 nm. Thus we cannot *a priori* impose the formation of interfaces but desire to predict the formation of steep but continuous gradients that experimentally will appear as interfaces. Models such as the GRAAL model do impose the formation of interfaces and use these to predict the components leached to solution. Consequently, these models cannot predict the experimental results from TOF-SIMS or APT data nor provide insight into why interfaces and layers are observed experimentally.

Model Transport

In experimental studies of glass dissolution, heat transfer or chemical transport by convection or advection are not relevant. In addition we presume no pressure or electrical gradients exist within the glass that could drive transport. Transport only occurs by diffusion and thus the time change of each species is given by

$$\frac{dC_i}{dt} = D_i \frac{d^2C}{dx^2} + S_i \quad \text{Eqn. 1}$$

where the diffusivity (D_i) of many species such as networked SiO_2 or NaBO_2 are immobile. Partially hydrolyzed entities such as $\text{R}=\text{Si}(\text{OH})_2$ are also immobile. The source term (S_i) accounts for chemical reactions which are discussed in more detail below. Thus transport in glass is essentially trivial from a governing equation perspective [40].

There are two major difficulties. First, D_i depends upon other species and clearly diffusivity in water filled porous silica will be similar to that of pure water while that in pristine glass will be orders of magnitude smaller. A rigorous Maxwell-Stephan approach to estimating the diffusivities requires more knowledge about glass transport than presently available [43, 44]. On the other hand, Fickian diffusion where D_i is constant and independent of local composition is clearly not relevant [41]. Tomozawa [25-29] and Zhang [30-34] have suggested from experimental data that the effective diffusivity of water in glass is proportional to the water content. Thus we use the equation

$$D_i = D_i^0 (X_{\text{H}_2\text{O}})^p + D_i^{\text{gls}} \quad \text{Eqn. 2}$$

to describe how the diffusivity varies with water content. It is a major objective of this work to explore how this equation and the value of exponent, p , influence the distribution of species and to address if this aspect of the model allows us to predict the formation of interface-like gradients.

The second difficulty lies in the imposition of zero pressure and electrical potential gradients. Pressure gradients can arise from changes in partial molar volume as well as diffusive transport. We make the assumption that all oxygen containing species have a molar volume proportional to their oxide content and maintain a constant oxygen mass per unit volume. Thus SiO_2 occupies twice the volume of H_2O . In reality there are significant molar volume changes but at this stage of model development, the mathematical simplification justifies this assumption. Oxygen mass balance is maintained by using H_2O to fill all space left vacant by diffusion. Thus water is not considered to diffuse but rather is created or destroyed to maintain total oxygen mass balance.

This approach results in one problem in that water diffusion into pristine glass cannot be strictly modeled. We overcome this problem by assuming some of the oxygen sites (not to impose the concept of a lattice) are vacant. A vacancy or "Free" species is allowed to account for one oxygen atom in the mass balance, is allowed to diffuse out of the glass according to Eqn. 2 and is supplanted by one H_2O .

In addition the chemical reactions described below create mobile anions and cation such as Na^+ or H_3SiO_3^- and it is necessary to maintain electrical neutrality. This is done by adding H_3O^+ or OH^- as needed to maintain charge balance and ensuring water dissociation equilibrium

$$K_w = \frac{[H_3O^+][OH^-]}{[H_2O]^2} \quad \text{Eqn. 3}$$

$$[H_3O^+] = [OH^-] = \sqrt{K_w} [H_2O]$$

Note that the equation for K_w has $[H_2O]^2$ in the denominator [45] and thus is somewhat different than the more common equation but allows water equilibrium to be imposed at low total water concentrations. The second equation defines a “neutral” solution corresponding to pH 7 in bulk water systems.

With equations for total oxygen mass balance, charge balance and water equilibrium it is possible to eliminate the need for pressure and electric potential equations which are much more difficult to numerically solve.

Source and Sink Terms – The Chemical Reaction Set

It is conceptually possible to propose an almost endless set of chemical reactions that probably occur to some extent in glass corrosion. One could for example break the hydrolysis of SiO_2 into four separate reactions with each adding a silanol group until the mobile H_4SiO_4 species is formed. Since only the last hydrolysis product is mobile we treat the reaction as a single step from SiO_2 to H_4SiO_4 . From NMR studies for example the species formed within the glass from the original oxide melt can be proposed. [18-24] Thus we know that, as a simplified rule, Na first associates with Al to form $NaAlO_2$ and then with B to form $NaBO_2$ and finally any remaining Na forms $NaSiO_{5/2}$. From the original oxide composition of SON68, we calculate the speciation and use these as the entities which undergo hydrolysis. In addition, it is necessary to account for dissociation of acids such as H_4SiO_4 and H_3BO_3 .

The set of chemical reactions considered in the model could and should be of vigorous debate. However, our purpose is to define a minimal reaction set that accounts for the depth profiling data. Since TOF-SIMS and APT give only elemental information, we make the initial assumption that only the species present in the pristine glass and the mobile species formed through hydrolysis are important. In addition select acid/base reactions are included. The reactions considered in this model are listed in Table 1. These differ from those listed above in that acidic species are allowed to ionize to an extent determined by the individual pKa values and alkali-ion pairs are allowed to fully dissociate.

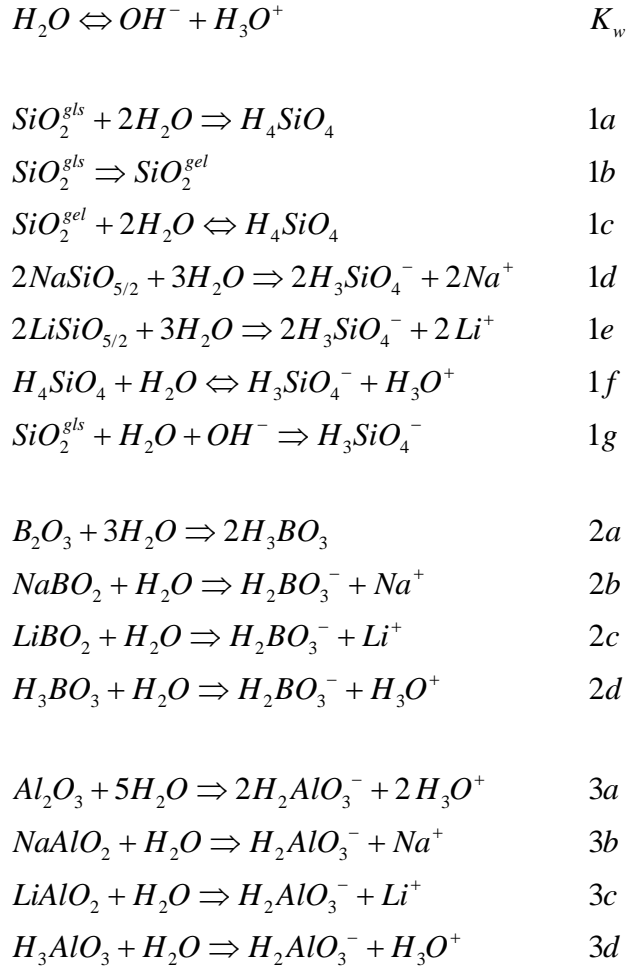


Table 1. List of Chemical Reactions Considered in the Model.

A problem results in that SON68 contains many other oxides not listed in the table such as Cs_2O , Fe_2O_3 , CaO and many others. Species such as Fe_2O_3 probably behave like Al_2O_3 and are relatively unreactive. Others such as Cs_2O probably behave like Na and are rapidly hydrolyzed to the mobile cation. Ignoring reaction and diffusion of these species reduces the local water content and reduces the reaction rate of the species that are considered. On the other hand it is mathematically simpler to ignore these oxides and assume all other oxides are replaced with SiO_2 (keeping the oxide mass constant of course) and adding species to the model as desired. More importantly this simplifies the construction of the model in that the very minimal system consists of SiO_2 , Free and H_2O . H_3O^+ and OH^- are easily to add to this baseline model. We then add B_2O_3 and $NaBO_2$ as well as $LiBO_2$ if desired. Finally we have added Al_2O_3 , $NaAlO_2$, and $LiAlO_2$.

Each chemical reaction requires either imposition of equilibrium or a forward rate, a reverse rate and an associated equilibrium constant which are related by

$$k_{rev} = \frac{k_{for}}{K_{eq}}$$

Eqn. 4

Many of the reactions in Table 1 are irreversible and this condition is imposed by setting K_{eq} for that reaction to some large value. By trial and error setting $K_{eq} = 1000$ gives a suitable approximation to irreversibility. The forward rate constant is then adjusted to obtain the desired result. In some cases the equilibrium constants are linked through a series of reactions. The $\text{SiO}_2(\text{gls})$, $\text{SiO}_2(\text{gel})$ and $\text{H}_4\text{SiO}_4/\text{H}_3\text{SiO}_3^-$ systems are one example.

While the transport equations involve only one parameter, i.e. the power dependence of diffusivity on water content, the source sink terms add a large number of parameters. The skeptical reader might suggest that we can now fit the model to anything. Such would be the case if only the solution composition data were available as was the case until recently. The depth profile data in combination with the isotopic swap scheme provide a huge amount of data that warrants a more complex model. However the model developer is well aware of the need to identify a minimal chemical reaction set which can explain the data but does not over parameterize the model.

Selected Results

Below we present select results that illustrate the capabilities of the model. The model as implemented in the PDE solver is one dimensional and has a length of 1.0 meter. In addition, each execution of the model was run for 1 s. Historically these types of simulations are conducted on dimensionless forms of the equations. However, the COMSOL PDE solver prefers a set of standard units and does unit checking that helps resolve typographical and logical errors. The results can then be scaled by length and time factors for direct comparison with experimental data. Of course a single

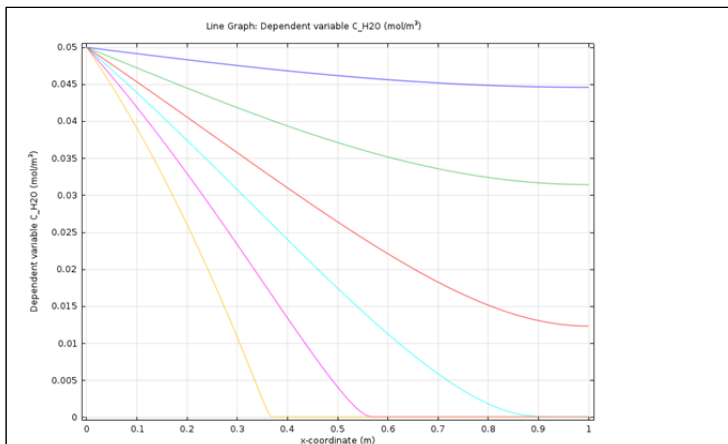


Fig. 1 Influence of the parameter p from Eqn. 2 on the diffusion of free vacancies out of a purely unreactive silicate glass. The curves from top to bottom correspond to p values of 0.0, 0.2, 0.4, 0.6, 0.8 and 1.0.

set of scaling factors must be used and it is not acceptable to scale the model for one experimental data set differently than for another.

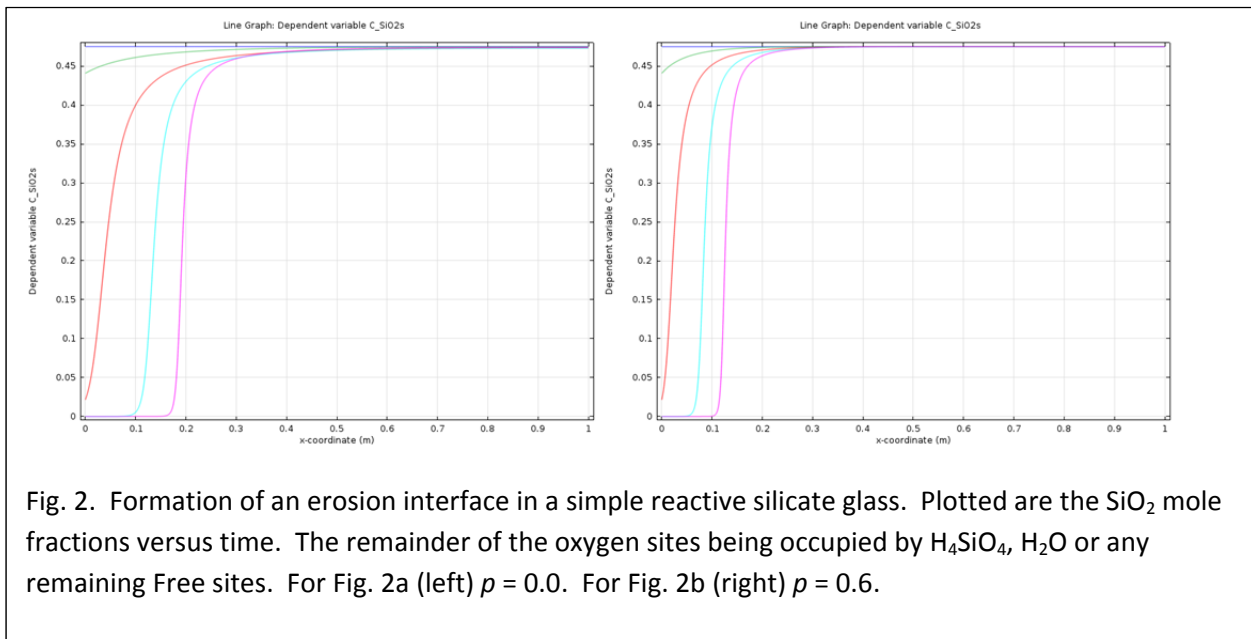
Our purpose here is to demonstrate that we can achieve behavior that accounts qualitatively for the formation of the five regions discussed in the introduction.

Dependence of Diffusivity on Local Water Content

The power factor, p , in Eqn. 2 has a substantial influence on the diffusivity of species and on numerical stability of the model. Fig. 1 shows the influence of p for simple diffusion of “Free” vacancies out of the glass into solution where they are destroyed. H_2O makes up the

difference. It was assumed that 95% of the oxygen sites were occupied by SiO_2 leaving an initial concentration of Free sites of 0.05 mole fraction. The upper most blue line is for $p=0$ which is the behavior expected for simple Fickian diffusion keeping in mind that the right hand side is a no-flux boundary and that material accumulates. The remaining lines are for $p = 0.2, 0.4, 0.6, 0.8$ and 1.0 . Note that for the latter two values of p , the mole fraction of water drops more or less linearly to zero where it sharply levels off to a small baseline value. This sharp inflection results in numerical instability and for more complex systems it was necessary to incrementally increase p using the previous solution as a starting point. The important point is that with $p < \sim 0.6$ there is only a gradual gradient of water content while with larger values the glass has a pristine region and a hydrated region with a distinct inflection separating the two. This behavior will continue to be observed in model runs described below but with added complexity as chemical reactions are included.

Formation of an Erosion interface



Figs. 2a and 2b show the formation of a dissolution interface. It was accomplished by setting K_{eq} for Reaction 1a from Table 1

to 1000, i.e. it is irreversible, and then increasing the forward rate constant until the concentration curve reached zero at some time. In this case, it was at about 0.5 sec but time is relative here. More importantly at 1.0 sec a fairly sharp interface is present at $x \sim 0.2$ m. For the simulation of Fig. 2a, with $p = 0$, the diffusivity does not depend upon water content. The rate of erosion appears to decrease with time.

Fig. 2b shows a similar result for $p = 0.6$. The interface has moved closer to the zero point and is somewhat sharper. For our purposes solving for the $p = 1.0$ condition would have been quite laborious and involved solving the problem while incrementing both the p value and the forward reaction rate constant. The value here was in determining values for K_{eq}

and k_{for} that result in at least minimal erosion. In comparison both simulation show the erosion rate decreases with time but is slower for higher values of p .

In summary, these results show that erosion can be successfully implemented in the model.

Formation of the Gel and Transition Layers

Fig. 3a and 3b show the results for a system that includes the reactions relevant to water, silicates and borates. Specifically Rxns. Kw, 1a, 1f, 2a, 2b, 2d from Table 1 are considered. In this case the reaction rate for hydrolysis of silica was reduced to prevent erosion and to focus on silicate, borate and sodium reactions and transport. There is considerable information and unique behavior in this plot and we discuss the features in detail. But first the reader should note the red, black, green and blue marker arrows at approximately 0.1, 0.2, 0.4 and 0.5 m. As the key is not very clear, the red line is the total Silicon content, the magenta is for Boron, the blue for Sodium and the green for water species. Fig. 3a is a log plot while Fig. 3b is a linear plot of the same data. The plots show a single point in time at the end of the simulation. The temporal transition to the distribution shown in the figures is beyond the scope of this discussion.

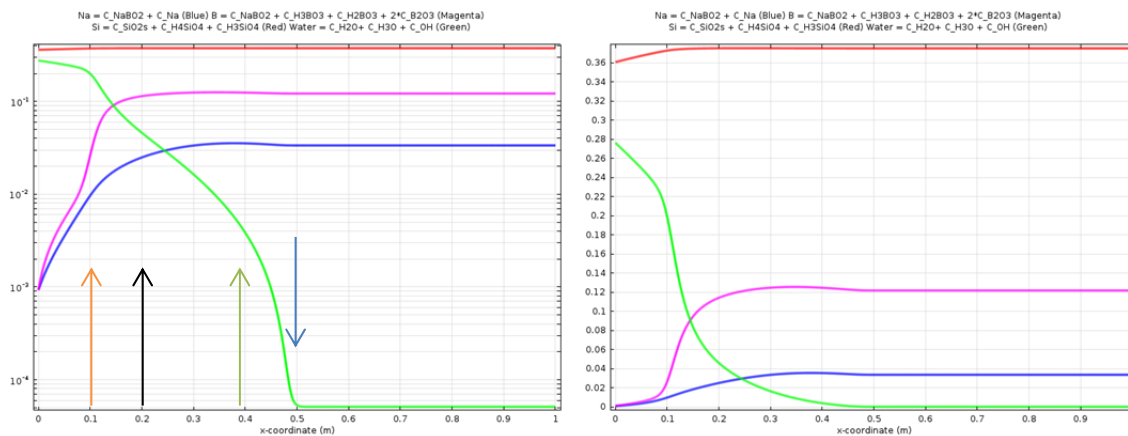


Fig. 3 Elemental distributions at $t=1.0$ sec for Si, B, Na and H_2O . See text for details

Region 0 – Not present

In this case, the glass was not allowed to erode to any significant extent such as that shown in Fig. 2. This is mostly a practical computational issue. Long computation times result from combining too many physical phenomena.

Region 1 – $0 < x < 0.1$ m, to Red Line

The Silicon content remains essentially constant except for a drop near the surface but it maintains its bulk value for $x > 0.1$ m. The water content, mostly H_2O but some OH^- and H_3O^+ is significant in this near surface region. Meanwhile the Boron and Sodium contents drop by more than one order of magnitude in this region and the linear plot shows clearly that this region is depleted of Boron and Sodium.

Region 2 – $0.1 < x < 0.2$ m, to Black Line

The black arrow denotes another transition in behavior of the curves. In this region, the Boron content begins to drop from the bulk value to about 10% of the bulk value as is more apparent in the linear plot. Meanwhile the water content drops by an order of magnitude but in the opposite direction.

Region 3 – $0.1 < x < 0.4$ m, to Green Line

In region 3 the sodium content drops from its bulk value to a near zero value at 0.1 m. The water content again drops by another order of magnitude. Actually region 3 is not distinct from region 2 but overlaps and includes region 2. The difference is that Sodium depletion extends over a greater distance than Boron depletion.

Region 4 – $0.4 < x < 0.5$ m, to Blue Line

In Region 4 the elements remain at their bulk values and the water content drops to the baseline level. (Approximately 100 ppm water was included in the pristine glass.) Thereafter the glass is that of pristine glass.

Region 5 – $x > 0.5$ m, Blue Line

This is pristine glass.

Discussion

From these results it is clear that by judicious choice of diffusivities and reaction rates we can produce elemental profiles that are in qualitative agreement with depth profile data and demonstrate the formation of apparent interfaces. Yet this was accomplished using continuous mass transport equation and reaction rates that under normal circumstance would not produce interfaces. The key is the non-linear model of diffusivity combined with the observation that diffusion of a species out of the glass, which is more rapid nearer the surface, results in greater water content and hence faster hydrolysis and faster diffusion.

Region 0 corresponds to erosion although we have not moved the interface and the associated boundary conditions. However, the complete depletion of silica and other species clearly resembles erosion but the interface with Region 1 is somewhat diffuse.

We propose that Region 1 corresponds to what is normally referred to as the Gel Layer. It consists primarily of silicates and is depleted of Boron and Sodium. As most of the Boron or Sodium found in solution will come from either the eroded layer or this nearly completely depleted gel layer the mass of Boron and Sodium in solution would be in approximate proportion to their glass mole fractions. Thus Boron and Sodium dissolve “congruently”.

Regions 2 and 3 are actually a single region, which we rename Region 23, in which water is in sufficient supply to hydrolyze the oxides and to accommodate slow diffusion. Diffusion increases rapidly as the water content increase

nearer the surface and rapid depletion of Boron and Silicon is observed. The important feature of this region is that the boundaries are not well defined and depend distinctly upon the reactivity of each glass component.

Region 23 corresponds to what the author refers to as a transition region and might be correlated with what the French workers call the Passive Reactive Interface (PRI). This authors understanding of the PRI concept is that this interface - or more properly this region – has limited hydrolysis and diffusion and may be the rate limiting process in glass corrosion. Again because the diffusivity is nonlinear and chemical reaction consumes water, reaction and transport in this region slows dramatically.

Since mobility is limited in Region 23 but there is still some water present, this may be a region where the silica in glass may undergo rearrangement to form a more stable gel material. (Note that the use of the term Gel Layer and the formation of a specific stable silicate material often call a gel are not necessarily the same thing and can be confusing.) This process has not been modeled here but the model can easily be adapted to included rearrangement. The silica to gel rearrangement would not consume water but presumably would be catalyzed by water. Most importantly, we do not understand how diffusion would change due to this transition. If the gel material aggregates to form a dense silica rich layer it could impede diffusion dramatically.

Region 4 might be considered to correspond to the Ion Exchange Layer but the model does not currently handle ion exchange realistically. However it is in this region where the water content is dropping to the background level of water in glass (some as silanol groups) and solid state diffusion of H^+ , Na^+ and Li^+ , sans hydration spheres, is likely to occur. Eqn. 2, describing the dependence of diffusivity of a species on water content, has a constant residual term that corresponds to solid-state diffusion when the water content is negligible. We would expect this residual term to be greater for Li^+ than for Na^+ . Presumably H^+ is even slower as it will bind more strongly to oxygen lone pairs. In addition, electroneutrality will force the diffusivity to depend upon the diffusivities of both cations involved in exchange. This aspect of the model has not been examined in detail but the model framework will allow its inclusion.

Conclusions

A model of glass corrosion has been developed using physically and chemically sound principles of transport and reactivity. The diffusivity of mobile species, presumed to be dependent upon the local water content, and a simple power dependence, based upon experimental studies, is used here. A minimal chemical reaction set is used for the source sink terms in the governing mass transport equation.

By appropriate choice of equilibrium constants, some well-known, and reaction rates as well as the power dependence of the diffusivity, elemental distributions within the glass could be predicted. The elemental profiles were demonstrated

to reproduce qualitatively the features of TOF-SIMS and APT data and could be correlated with mechanistic concepts that propose the formation of interfaces within a corroding glass.

Future Work

The width of each of these regions and the concentration profiles will depend strongly on the choice of chemical reaction rates. We do not yet have sufficient experience to manipulate the profiles at will and need to explore this in more detail. Once a preliminary set of reaction rates has been identified, these can be refined by comparison with the experimental APT and TOF-SIMS data. These refined values can be further quantified by using the GCMT to compare the time dependent model with the time dependent experimental data.

The nonlinear diffusivities result in very “stiff” equations and direct single pass solutions are generally not possible. The desired solution must be approached starting initially with simpler chemistries and more linear dependence of diffusivities and allowing the solution to build to the desired complexity. It is possible to solve the model for a LiNaAlBSiO_x glass in a matter of a couple of minutes if $p=0$, i.e. the diffusivity does not depend upon water content. However as p approaches 1.0, the solvers become unstable and increasingly finer meshes, smaller time steps and smaller parameter increments are needed.

An ultimate objective is to model the isotopic swap experiment conducted on SON68 glass at PNNL. However each isotope represents a new species that must be included. While the reaction rates and diffusivities won't depend on the isotope, the concentration profiles will be important at the point where the differently labeled glasses were swapped. For some elements, data is available for 3 or even 4 isotopes. The number of model components could easily increase by a factor of two, if not more.

Finally, the model currently assumes the concentration of each soluble species is zero at the solution interface. This does not allow us to make full use of the ICP data for the solution composition. To modify the boundary conditions to reflect changes in solution composition the flux of each species across the interface must be tracked. Some preliminary work has been done to include this in the model but has not been fully implemented. This aspect will be important in modeling the isotopic swap experiments as the solution represents a source of isotopes which will diffuse into the glass.

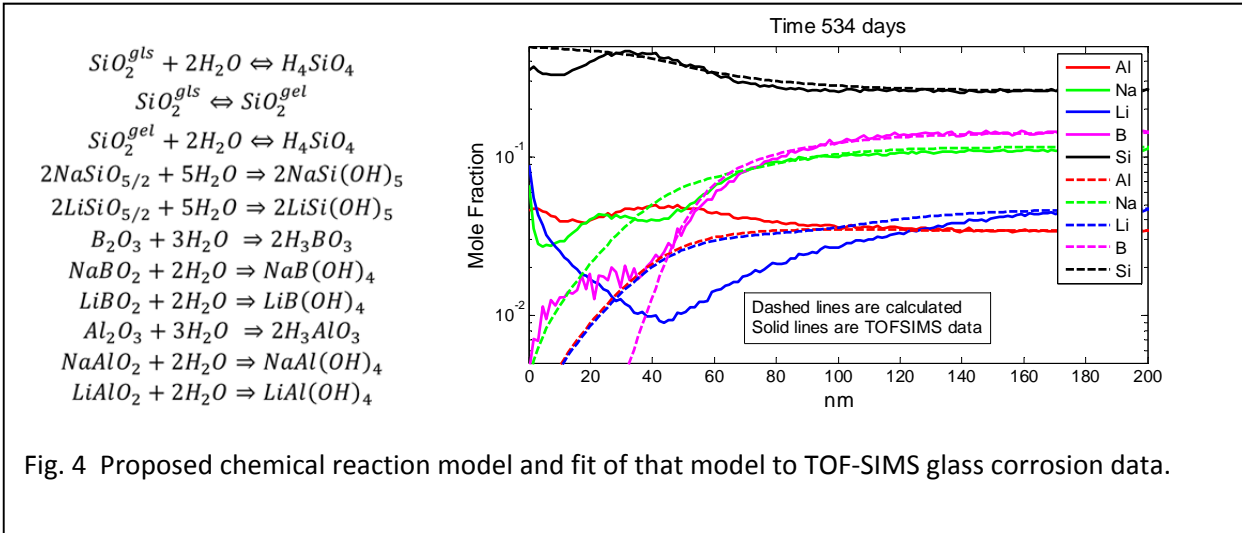
New Applications

Modeling Depth Profiling Data

PNNL has utilized static tests in combination with isotopic labeling experiments and TOF-SIMS and APT analysis techniques to characterize the corrosion of nuclear waste glasses. These have provided unparalleled nanometer

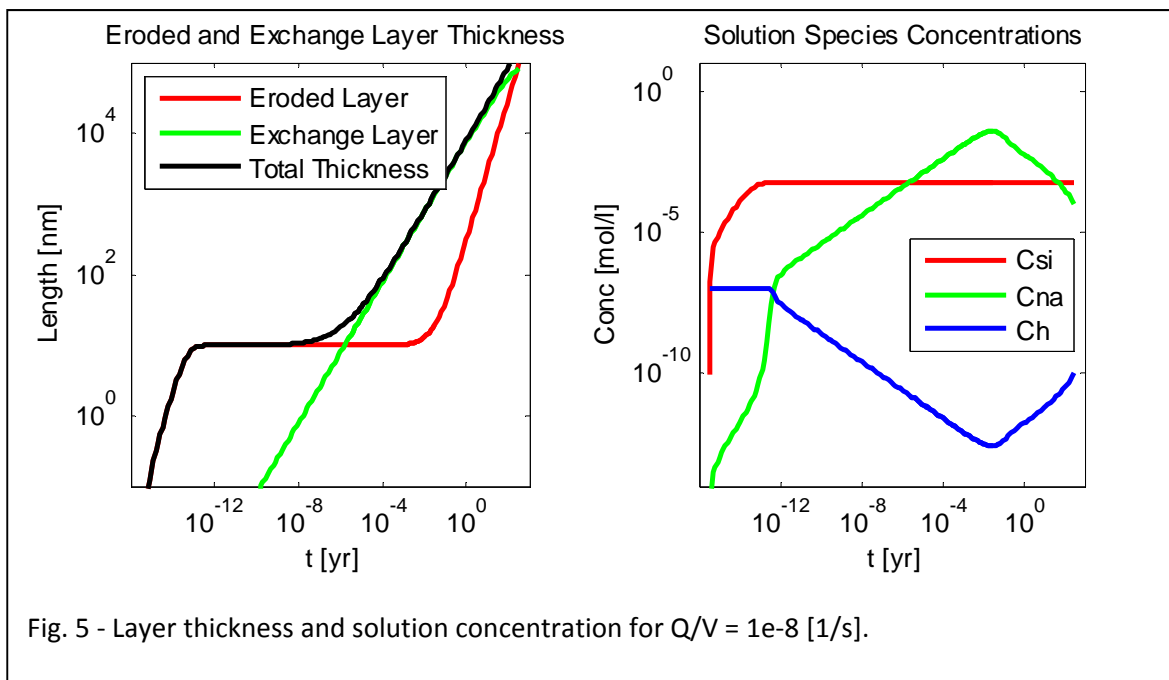
resolution depth profiles of the elemental distributions within the glass. Above we briefly outlined the DCRx model and report here on the initial analysis of the TOF-SIMS data using the GCMT to fit the model parameters.

Figure 4 illustrates how the GCMT was used to model TOF-SIMS data and the associated chemical reaction set. In brief summary, that glosses over many fine points of the analysis; the model does an adequate job of explaining Na, Si and B



leaching but fails to even qualitatively describe how Al and Li are leached from the glass. To remedy this deficit, the model will need to be modified to account for how $Al(OH)_4^-$ and/or related Al species are bound to the leached portion of the glass. While Li^+ is not expected to bind strongly to leached glass, the comparison of model and data suggest that solid state diffusion may be important for Li^+ .

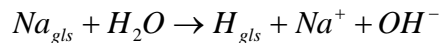
We note that TOF-SIMS is considered semi-quantitative because of unknowns in the sputtering rate. However these



results illustrate that even a poor qualitative fit provides significant information on how to modify the proposed dissolution mechanism and an improved model can be proposed and tested with the GCMT. This basic model and improved models will be more fully tested once the ICP and APT databases can be fully accessed by the GCMT.

Residual Rate Effects in ILAW Glasses

Workers at PNNL are considering new experiments to study corrosion of Immobilized Low-Activity Waste (ILAW) glasses. The role of “Residual Rate” corrosion is important in this task and to address this issue the GCMT was used to compare the Constant Residual Rate (CRR) and the GRAAL models. Both assume the exterior layer of glass is eroded (i.e. completely dissolved) at some rate controlled by the pH in solution as well as the degree of saturation with respect to a silica gel phase. They differ in that a second term describing how the glass is more easily leached of some species, such as Na and B, leaving behind an altered layer. In this instance interest was in the ion exchange process



where the release of sodium results in a rise in the pH of the solution and this may increase the rate of dissolution.

Figure 5 show a typical result for analysis of the GRAAL model using rate constants reported by Bacon and McGrail (PNNL-15198) for LAWA44 glass [14]. The objective here was to explore if the exchange layer growth influences the eroded layer thickness. Elements of interest such as radionuclides will be released depending upon how strongly they bind to glass. This behavior is a result of the assumptions behind the GRAAL model. The GRAAL model essentially models release as two congruency patterns. In reality each species would be released from the exchange layer in a slightly different manner and thus would not be entirely congruent with each other.

From these results, the release of radionuclides may or may not be associated with the residual rate as determined by the exchange layer growth rate. It is clear that ion exchange influences pH but more weakly influences the degree of super-saturation of silicon with respect to a rather nebulous equilibrium constant for the silica gel like material left after alteration. In the limited solution chemistry model used here, pH does not influence the rate of dissolution or exchange. Simply stated, the solution comes to saturation so quickly that the rate of approach to saturation is unimportant.

However dilution of the solution by flow has a much more significant influence. While the solution remains saturated with respect to glass/gel material, the dissolution exactly matches that of dilution by flow resulting in a constant dissolution rate. The exchange layer thickness becomes constant because the rate of dissolution matches that of ion exchange.

Appendix A. Preliminary User Manual

Introduction

The Glass Corrosion Modeling Tool or GCMT allows the user to evaluate the goodness of a glass alteration model by fitting the model to a selected experimental database. It returns the best estimate of the model parameters. The GCMT allows comparison of different models and ultimately allows a scientific method of choosing the best possible model. By this means researchers can understand how particular models succeed or fail in explaining certain results and allow them to modify the models on a rational basis. Engineers can use the tool to quantitatively justify the choice of a certain model of glass dissolution and the associated parameters values used in the model. Those models can then be used in codes used to predict the durability and lifetime of nuclear waste packages.

Analysis of a model against a particular database consists of three steps implemented through MatLab. The first step is to import the desired data from various data sets usually in the form of Excel spreadsheets. The next is to select a particular model of glass alteration and these are discussed in detail below. Each model is implemented in a different manner and these differences are discussed below. Finally the PEST package is used to fit the data to the model. From that the user can extract plots of the fits as well as statistical data on the fits. Examples of use of the code are include in the appendix or can be obtained from the authors.

Currently the GCMT incorporates three established models of glass alteration and a fourth Diffusive and Chemical Reaction (DCRx) based model. The Aagaard-Helgeson (AH) [46], Grambow-Muller (GM) [47] and the "Glass Reactivity with Allowance for the Alteration Layer" (GRAAL) [10-12] models are implemented. The AH and GM models are linear, algebraic equations and were coded as MatLab functions. The GRAAL model is a set of non-linear partial differential equations (PDE) which were implemented with the COMSOL PDE solver. PhreeqC was used as needed to solve for solution compositions and to calculate pH values. The AH and GM models are time independent while the GRAAL model allows the time dependence of glass alteration to be modeled. The fourth DCRx model is based upon more fundamental physical and chemical effects in the glass but which are significantly different from those found in "reactive transport" codes which implement specific chemistries relevant mostly to ground water transport. The physical details behind each model are discussed in detail below.

A number of sources of glass corrosion data can be imported into the GCMT and interfaces are provided to import specific databases and to down select specific data sets. Unfortunately most databases require a tailored interface and new databases will require adaptation of the import routine. Most of the existing databases report only concentrations of elements dissolved into solution but sometimes the original workers have manipulated the data using some theoretical assumptions that are often not clear but were at the time appropriate to the understanding of glass

corrosion. TOF-SIMS and APT data can also be imported although these need extensive manipulation to be converted into local mole fractions appropriate to the model being analyzed.

Finally not all data is appropriate to a given model. For example, TOF-SIMS depth profiles cannot be predicted by the AH, GM or GRAAL models and the new TCRx model is needed. The AH and GM models are not time dependent and hence are not relevant to the quite common single time point dissolution tests.

Obtaining Using the GCMT

The GCMT development is still in a state of flux and a fully user friendly GUI interface is not yet available. Further the GCMT has as of yet been only used by the author and is in need of testing by knowledgeable outside users with the aid of the author. Should you have interest in the GCMT please contact the author. The contact information is:

Peter C. Rieke, Ph.D

Pacific Northwest National Laboratory

Richland, WA 99354

Peter.rieke@pnnl.gov

509-375-2833

The GCMT is a set of MatLab routines that makes calls to other software packages and was developed using MatLab 2013b. However, no special packages were used and the basic MatLab package should be adequate.

The parameter optimization package, PEST, can be obtained free from <http://www.pesthomepage.org/Downloads.php> . Version 13.0 was used in this work.

The AH and GM models are implemented as MatLab routines and no additional software are required to analyze these models unless the user wants more information of solution speciation using PhreeqC

The IPhreeqC module can be obtained from http://wwwbrr.cr.usgs.gov/projects/GWC_coupled/phreeqc . Only the IPhreeqC module is required but the PhreeqC and GUI packages can be useful in understanding how PhreeqC works. Various thermodynamic databases can also be obtained from this site. The llnl.dat database was used in most of this work.

The GRAAL and DCRx models are implemented in COMSOL as 1D problems using the Coefficient Form PDE physics. These models can be obtained from the author as “mph” files for use with the COMSOL GUI but would not be directly applicable to the GCMT. The “m” or MatLab version of the files is required for the GCMT and their implementation is

controlled by MatLab. The basic COMSOL and MatLab LiveLink package are needed. These can be obtained from COMSOL at <http://www.comsol.com>.

The ALTGLASS database can be obtained from Dr. Carol Jensen at Savannah River National Laboratory. The database has not yet been formally released and she would like to keep tabs on who has which version. She can be contacted at carol.jantzen@srnl.doe.gov. Other databases can be obtained from the author.

Overview of the Mechanisms of Glass Alteration

The glass alteration literature is very extensive and from this a variety of mechanisms of dissolution, leaching, swelling, and precipitation have evolved. Often these observations are interpreted in terms of “layers” formed in the glass and as discussed further below many models of glass corrosion are based upon formation of these layers to explain the dissolution rate of various elements [9, 11, 35-39]. (Side note: By “mechanism” we refer to a non-mathematical description of some or all physical and chemical phenomena. By “model” we refer to a mathematical implementation of some set of mechanisms.) Our purpose here is to provide a tool, the GCMT, to test models against experimental data, identify shortcomings of the model and allow the user to suggest model improvements. This brief overview of glass alteration mechanism is intended to provide a basis for discussion of the models and not to be a review of this field.

For discussion purposes we focus on Sodium Aluminoborosilicate (SABS) glasses that may also contain lesser amounts of other elements. From structural experimental data, such as NMR, these elements have distributions that are not entirely random and some elements associate closely with other. For example Boron tends to form clusters; while most Sodium prefers to be associated with Aluminum.

It is generally accepted that water both diffuses through and reacts with the glass constituents at rates highly dependent on local composition. It is also generally accepted that singly charge ions such as Na^+ , Li^+ or H^+ may diffuse through the pristine or non-hydrated glass and have a diffusivity greater than that of H_2O . Highly charged cations, e.g. Ca^{+2} , do not diffuse to any extent until local water concentration become significant. Boron and Sodium react with water rapidly and tend to leach “congruently” in that the ratio of their concentrations in solution tend to track that in the original glass. This is not to say they are released by the same mechanism.

Species diffuse from the glass into solution at a rate highly dependent on local structure and in particular on the local water content. Thus species diffuse rapidly near the open and porous surface of the glass and much more slowly deeper within the glass until the diffusivity is that of the dry glass. The end result is that the altered glass forms “layers” because once diffusion reaches a certain level it speeds up as the water content increases and chemical reaction rates increase. The result is the formation of apparent boundaries between layers given descriptive names such as “gel layer” and “Passive Reactive Interface” (PRI).

Silica plays a unique role in being the major species but also in undergoing slow hydrolysis compared to say Boron. Silica is assumed to dissolve and precipitate either outside the glass as a mineral phase or within the glass as some amorphous “gel” phase of indeterminate and changeable composition. However the gel is often assumed to have a definable solubility constant as though it were a mineral phase with a defined composition. Recently, it has been proposed that silica undergoes rearrangement (as opposed to reprecipitation) to form the gel phase.

We have purposefully glossed over details of these proposed mechanisms because it is apparent that most models of glass dissolution impose *ad-hoc* formation of layers, assume some congruent or non-congruent leaching from each layer and predict the observed amount of each element in solution. Still it is apparent that from a mechanistic stand point, that the alteration of glass is essentially quite simple in that transport consists of simple diffusion with no convective transport (except in the adjoining solution which is usually “well-mixed”), no significant thermal gradients arising from the heats of reactions and a set of chemical reactions that may or may not be multistep. The key issues are 1) identifying the fundamental set of chemical reactions, 2) proposing rate constants for these dependent on local composition predominately driven by the local water content, and 3) proposing how the diffusivity of mobile species depend upon local composition.

The partial differential equations needed to describe such a system are essentially mathematically simple. However the key issues represent “constitutive” relationships that must be proposed, describe in detail and widely presented to the community. To date these constitutive relationships have been largely ignored from a modeling perspective.

Description of Models

The basic premise and applicability of the Aagaard-Helgeson, Grambow-Muller and GRAAL models are described below. We also discuss the DCRx model under development.

The Aagaard-Helgeson Model with Residual Rate [1-3]

The Aagaard-Helgeson (AH) equation was developed to describe dissolution of minerals [46] and is largely based upon kinetic rate theory developed by Eyring [48] and simultaneously by Evans and Polyani in the 1930’s and more recently review by Laidler [49]. Gin et al. have reviewed the development of the theory and its application to glass alteration [50].

The Aagaard-Helgeson equation is

$$r_i = k_{gls} h_i a_{H^+}^{-\eta} \left(1 - \frac{a_{SiO_2}}{K_{gls}} \right) \quad r_i \left[\frac{mol_{elem}}{m^2 s} \right] \quad k_{gls} \left[\frac{mol_{gls}}{m^2 s} \right] \quad h_i \left[\frac{mol_{elem}}{mol_{gls}} \right]$$

$$k_{gls} = k^0 \exp\left(-\frac{E_a}{RT}\right) \quad K_{gls}^{T_2} = K_{gls}^{T_1} \exp\left(-\frac{\Delta H^\theta}{R} \left(\frac{1}{T_2} - \frac{1}{T_1} \right)\right)$$

where the rate of dissolution for a species such as Al, B, Na or Si is proportional to the overall glass dissolution rate and the appropriate mole or mass fraction. It is more convenient for our purposes to express this on a molar or molality basis rather than on a weight basis. The temperature dependence of the glass dissolution rate constant is described by the Arrhenius equation while that of the glass equilibrium coefficient is described by the van't Hoft equation. In the above equation, the dependence on pH is given by the $a_{H^+}^{-\eta}$ term. Additional terms may be added, such as that for the hydroxyl concentration, as well as other species in solution but the latter are usually ignored.

The fundamental limitation to the model is that it assumes a reactive interface where minerals transition from the crystalline state or the unhydrated solid state, in the case of glasses, to a completely dissolved state. Thus all dissolution is congruent. The model does not account for the formation of a gel layer, precipitation of minerals or other physical phenomena thought to be important in glass alteration. Too partially account for continued alteration in the event of supersaturation a "residual rate" term is added and the above equations now becomes

$$r_i = k_{gls} h_i a_{H^+}^{-\eta} \left(1 - \frac{a_{SiO_2}}{K_{gls}} \right) + r_x$$

The AH model is reasonably successful in accounting for many dissolution data and was used by Pierce et al. to interpret the results of their large glass dissolution study [15, 51].

The Grambow-Muller Model [4-9]

The Grambow-Muller (GM) model was developed to account for the possible formation of a barrier gel layer that hinders water transport [47]. The model, as presented by the authors begins with an equation describing water transport

$$\frac{dC_{H_2O}}{dt} = D_{H_2O,eff} \frac{d^2 C_{H_2O}}{dx^2} - U(t) \frac{dC_{H_2O}}{dx} - k C_{H_2O}$$

$$C_{H_2O} = 0 \quad x > 0 \quad t = 0$$

$$C_{H_2O} = C_{H_2O}^0 \quad x = 0$$

which is not particularly useful in that data on water or hydrogen content within the glass is not usually available. However depth profiling techniques may provide this data. The $U(t)$ term describes the rate of glass dissolution and its development provides a model for glass dissolution. The authors assume that the AH model, see above, describes the dissolution of pristine glass at an “interior” interface. This interface is covered by a diffusive barrier layer that is formed at the glass/solution interface either by selective dissolution of some elements or by reprecipitation of silicic acid. Either way a “gel” layer is formed which impedes diffusion. A key assumption of the GM model is that the rate of glass dissolution at the pristine interface is equal to the diffusion of mass across the barrier layer as expressed by

$$-\phi D_{Si} \frac{m_{Si,sln} - m_{Si,int}}{L} \rho_{sln} = k_{gls} h_{Si} a_{H^+}^{-\eta} \beta (1-b) \left(1 - \frac{a_{Si,int}}{K_{gls}} \right) \quad a_{Si,int} = m_{Si,int} \gamma_{Si,int}$$

where the term on the left is the flux across the gel layer due to the concentration gradient and the term on the right is the AH model of dissolution at this interior interface. This assumption implies a steady state analysis and hence the GM model is not time dependent. The β and $(1-b)$ terms are included to account for surface area roughness and

accumulation of silicon in the barrier layer respectively. This equation is solved for $\frac{a_{Si,int}}{K_{gls}}$ keeping in mind that the

molality of silicon in the interior region is present on both sides of the equation. The end result is

$$\frac{m_{Si,int} \gamma_{Si}}{K_{SiO_2}} = \frac{\phi D_{Si} \rho_{sln} m_{Si,sln} + k_{gls} h_{Si} a_{H^+}^{-\eta} \beta L (1-b)}{\phi D_{Si} \rho_{sln} K_{gls} + k_{gls} h_{Si} a_{H^+}^{-\eta} \beta L (1-b) \gamma_{Si}} \gamma_{Si}$$

Substituting this back into the original AH equation, the dissolution rate for Si is given by

$$r_{Si}^* = k_{gls} h_{Si} \beta (1-b) a_{H^+}^{-\eta} \left(1 - \frac{\phi D_{Si} \rho_{sln} m_{Si,sln} + k_{gls} h_{Si} a_{H^+}^{-\eta} \beta L (1-b)}{\phi D_{Si} \rho_{sln} K_{gls} + k_{gls} h_{Si} a_{H^+}^{-\eta} \beta L (1-b) \gamma_{Si}} \gamma_{Si} \right)$$

However, if $L \approx 0$ the relationship reduces to the AH model

$$r_{Si}^* = k_{gls} h_{Si} \beta (1-b) a_{H^+}^{-\eta} \left(1 - \frac{m_{Si,sln} \gamma_{Si}}{K_{gls}} \right) \quad L \approx 0$$

and if L is very large the rate becomes zero. Grambow and Muller don't describe how the above equation can be used for other species such as boron or sodium, but we assume that dropping the $(1-b)$ term which accounts for silicon retained in the barrier layer results in an appropriate description. This is equivalent to saying the barrier layer does not capture any species except silicon but slows the transport of all species.

The GRAAL Model [10-12]

The GRAAL model [10-12] assumes the exterior layer of glass is eroded (i.e. completely dissolved) at some rate given by

$$\frac{dE}{dt} = r_E \left(1 - \frac{C_{Si}}{K_{gls}} \right) \quad r_E = k \frac{\rho_{gls}}{MW_{gls}} \left(\frac{a_{H^+}}{a_{H^+}^0} \right)^{-\eta} \exp\left(\frac{-E_a}{RT}\right) \quad (0.1)$$

where E designates the moles of glass eroded depending upon choice of units but can be converted to mass or thickness as desired. Note that dE/dt could have a negative value. This would represent deposition of some silica material that is most certainly not that of the original glass. This equation is, except for minor changes in form, equivalent to the AH model without the residual rate term.

An additional layer is also formed resulting in partial hydrolysis and leaching of the glass. This layer can be thought of as the gel, PRI or Ion Exchange layer depending upon the application at hand. For the purposes of discussion we refer to this as the X layer as it is important not to assign too much meaning to the mathematical implementation of this layer. We can write

The GRAAL model assumes the summed rate of growth of these layers are given by

$$\frac{dE}{dt} + \frac{dX}{dt} = \frac{r_E + r_X}{1 + \frac{X(r_E + r_X)}{D}} \quad (0.2)$$

When X is small, the second term in the denominator can be dropped and the equation reduces to

$$\frac{dE}{dt} + \frac{dX}{dt} = r_E + r_X \quad X \approx 0 \quad (0.3)$$

And the value rX represents a residual rate

If X is large such that

$$1 \ll \frac{X(r_E + r_X)}{D} \quad (0.4)$$

Then the equation reduces to

$$\frac{dE}{dt} + \frac{dX}{dt} = \frac{D}{X} \quad (0.5)$$

This result unfortunately ignores the growth rate of the eroded layer and is physically unrealistic. However it can be argued that X would be large only if

$$\frac{dE}{dt} \ll \frac{dX}{dt} \quad (0.6)$$

then the equation reduces to

$$\frac{dX}{dt} = \frac{D}{X} \quad (0.7)$$

By integration this equation shows that

$$X = \sqrt{2Dt} \quad (0.8)$$

And X grows with a realistic square root of time dependence.

In summary the GRAAL model better captures our understanding of glass alteration, the time dependence of the residual rate and the nature of diffusive transport than do the other models.

The GRAAL model focuses on changes in the width of the E and X regions and some assumptions are necessary to convert these to equations describing the release of the glass constituents. For Si and Na the change in concentration in solution contacting the glass is given by

$$\frac{dC_{Si}}{dt} = \frac{S}{V} C_{Si}^{gls} \frac{dE}{dt} - \frac{Q}{V} C_{Si} \quad \frac{dC_{Na}}{dt} = \frac{S}{V} C_{Na}^{gls} \left(\frac{dX}{dt} + \frac{dE}{dt} \right) - \frac{Q}{V} C_{Na} \quad (0.9)$$

In this model it is naturally assumed all glass constituents are release from the eroded or E layer but that some glass constituents are also released from the exchange or X layer. We write equations for Silicon and Sodium but similar equations can be written for any glass constituent. The original GRAAL model as presented by the French workers focused on Boron not Sodium. The second term in each equation accounts for solution flow which is assumed here to be pure water.

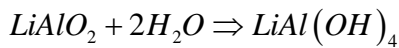
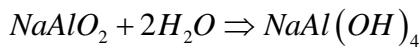
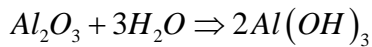
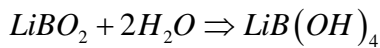
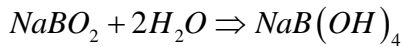
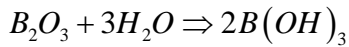
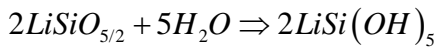
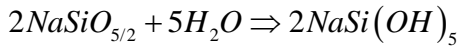
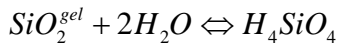
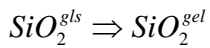
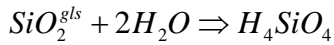
Diffusive Chemical Reaction (DCRx) Model

PNNL has utilized Single Pass Flow Through (SPFT), Time of Flight, Secondary Ion Mass Spectrometry TOF-SIMS and Atomic Probe Tomography (APT) to characterize the corrosion of nuclear waste glasses. These techniques in combination with unique isotopic exchange experiments have provide an unparalleled experimental examination of

glass corrosion with nanometer depth profiles of elements in the corroded glass as well as elemental and pH characterization of the contacting solution using Inductively Coupled Plasma (ICP) analysis.

The new depth profiling data described above cannot be modeled using existing glass corrosion models. A new model was implemented in the GCMT to remedy this lack. The model is based upon a set of reactions of immobile species found in glass, as for example from NMR data, and their reaction to neutral or ion pair species that are assumed to be mobile as described in more detail below.

The set of chemical reactions considered here are



All reactions are assumed irreversible except for the possible equilibrium of SiO₂-gel with H₄SiO₄. This model clearly ignores the formation of ionic species but provides a set of reactions that encompass the chemical possibilities. The model is extensible in that new secondary or intermediate reactions can be added as needed to explain experimental data.

The change in local concentration for each of these species is given by the conventional Fickian diffusion equation with an additional source/sink term, R_i , that is given by the sum of all reactions creating or consuming that species.

$$\frac{dC_i}{dt} + \nabla \cdot \left(-D_i \frac{dC_i}{dx} \right) = R_i$$

Of course the diffusivity of immobile species is taken as zero and that term drops out. The diffusivity of mobile species is assumed to be impacted primarily by the local concentration of water with a minimal diffusivity as determined by solid

state diffusion in the “dry” or pristine glass. This diffusivity of each species may be described by a power dependence of diffusivity on water content such as

$$D_i = D_i^{H_2O} (X_{H_2O})^n + D_i^{gls}$$

Where X_{H_2O} is the local mole fraction of water and $D_i^{H_2O}$ is the diffusivity in pure water and D_i^{gls} is that in dry glass. There are other rational approaches to determine the diffusivity but it is not clear if any are superior and we believe this is an adequate approach until the set of relevant chemical reactions is more clearly defined.

It is important to note that Fickian diffusion is not usually applicable as each of these species is not necessarily sufficiently dilute to ignore the mass imbalance that this would create. This problem is treated by considering water to be the only species which moves into a space left vacant by diffusion of a mobile species. In addition water must first diffuse into the glass to start the hydrolysis process but this may not be rate limiting. Water is considered to diffuse into the glass by a free volume model. In actuality this is modeled by diffusion of free volume “holes” out of the glass. These assumptions significantly simplify the transport and source terms in the partial differential equations (PDE) needed in the model.

The current focus is on incorporating ionic species that allows easy imposition of electroneutrality without resorting to a full description of charge distribution and the influence of ion mobility on electrical fields in the glass. The primary issue is that there is no dominant species that can be assumed to transport into a region to maintain electroneutrality. Hence diffusion of some ions will impact the diffusivity of other ions but on a local and specific basis that adds complexity to the model.

It is important to note that the transport equations for each species are applicable to nearly any system of chemical reaction with diffusive transport and can be amended to account for convection (advection) and multicomponent mass transfer. But these equations are not the basis of our model. The model of glass transport and reaction consist of our assumptions on the dependence of D on local water content, the set of chemical reactions (and rate constants) being considered and the treatment of water diffusion in pristine glass. These assumptions should and must be critically discussed at length.

Commonality and Differences

The AH equation is common to the AH, GM and GRAAL models as it is a fundamentally sound description of interfacial dissolution of a mineral with a distinct solubility constant. The problem is that the K_{gls} term (or equivalently C_{Si}^{Sat}) is not well known. Further, one can argue that the amorphous gel layer comprising the altered glass is not a constant composition mineral, is probably graded in composition, and may have a changing solubility coefficient. These

influences are ignored by all the models. The GM model and the GRAAL model differ in how formation of the altered layer occurs. The GM model emphasizes the reaction at the pristine interface and assumes formation of a gel layer which is referred to as a barrier layer while the GRAAL model focuses on dissolution at the water/glass interface and formation of an altered layer under this interface.

The major problem with both models is that formation of the altered layer - regardless of what name is given to this layer - is presented in a phenomenological approach and the models do not attempt to describe formation of the altered layer by the chemical or physical processes known to occur in this layer. In particular neither model incorporates the stepwise hydrolysis of silica or the influence of common glass constituents such as boron, sodium or aluminum. As a consequence these models cannot predict the depth profiling data provided by TOF-SIMS or APT.

Comparison of the DCRx and Reactive Transport

The term reactive transport is often used in the geochemical community to describe systems which undergo both chemical reaction and diffusive/ convective/advective transport. Codes like CrunchFlow, STOMP or HyTECH are reactive transport codes. COMSOL can also be setup as a reactive transport code and is used in the GCMT for its versatility and the ease of user interaction with the code. These are all PDE solvers while a model is a specification of the system of PDEs

In most cases the PDEs describing the change in mass with time are well established regardless of whether the system is a section of ground water, a distillation column or an electrochemical cell. The same fundamental physics apply. A model of any system consists of stating which abbreviated form of the fundamental transport equations will or will not be used in a particular instance. For example, electric potentials may be ignored by assuming electroneutrality. Or the Richards equation may be used to describe the flux of water into and out of porous space in soils. Alternatively, the Maxwell-Stephan version of the transport equations may be used instead of the simpler Fickian diffusion equations. These must be succinctly specified and any approximations clearly spelled out.

Further the exact set of chemical reactions and species which form must be delineated. PhreeqC for example can access a number of very large databases but usually the user limits the subset of species which are considered. Usually these databases are set up for aqueous systems and the chemical species may or may not be relevant to glass alteration.

Often transport coefficients such as the diffusivity or hydraulic conductivity are often assumed to be constant and independent of local composition. This is clearly not the case for glass alteration and any model of alteration must state the criteria by which these transport coefficients depend upon say water content or other factors.

The DCRx is a model of glass dissolution that specifies which fundamental physical transport equations are used, the approximations that may be made, the set of chemical reactions and species being considered and the dependence of

diffusivity on local composition. It is often difficult or impossible to determine what equations are being used in other “continuum” models of glass alteration. It is not sufficient to simply list the physics that are being considered.

As the DCRx is based upon a set of PDEs describing fundamental physics and chemistry, it is an extensible model. Any simplification can be relaxed or additional chemical reactions added as needed. This is in contrast to the AH, GM and GRAAL models which are phenomenological in that they may predict the correct dissolution rate of the glass, they do so by extending the equations beyond their applicability or impose non-physical assumptions on the rate of dissolution. This makes it difficult to modify them in light of new experimental evidence. The GRAAL model for example cannot predict TOF-SIMS or APT elemental distributions.

Databases available in the GCMT

Importing databases in to the GCMT is straightforward once the database has been translated from the original published format into a text file or spreadsheet. The approach used here was to import the data in the format provided by the authors and then manipulate the data such that the values represent that calculated by the model. For solution concentration data this is not difficult but requires attention to details the authors often leave out. For TOF-SIMS and APT data the manipulations are more intensive due to instrumental artifacts. TOF-SIMS for example is considered semi-quantitative because of unknown factors concerning the sputtering rate and hence the reported depth into the sample. This is not to say TOF-SIMS data should be ignored but that the model should predict general trends and not reproduce experimental detail.

The databases available at this time are

- 1) The time dependent SPFT tests on SON68 glass as reported by French workers[10]. The data are limited to Silicon, Boron and Aluminum and were originally reported in leachate solution concentrations and could be use directly with minor modification.
- 2) The extensive database reported by Pierce et al. [15, 51] which consists of five different LAWA glass compositions and three different experimental techniques. This data sets required development of code to extract the desired data, reverse the normalization applied to the data and convert the data to a consistent set of units. This data is not time dependent but the duration of the dissolution experiment is reported
- 3) The ALTGLASS data base prepared by Dr. Carol Jantzen at Savannah River National Laboratory. This dataset already in Excel format can be imported into the GCMT using a graphical user interface. The GUI allows rapid down selection of specific experiments based upon many factors including sample name, range of pH, time or times and experimental technique. The database currently contains about 2000 individual samples and more are being added. The data is mostly for a single leaching time that varies depending on the original author’s intent and experimental technique. However for some of the data three of four time points are available.

- 4) SPFT, TOF-SIMS and APT data for the time dependent isotopic labeling tests of SON68. The import routine is not yet complete and the APT data are missing but this should be available soon.

Examples of GCMT Uses

Example1. Optimizing the AH model against LAWA44 SPFT data

The AH model is the simplest possible model of glass dissolution and is often used to characterize SPFT data at a single time point. In this example we step through the GCMT main code and explain what each feature does. The entire code can be obtained from the author. MatLab, IPhreeqC, and PEST are required to run this example.

- 1) Initialize() deletes all files created in any possible previous analysis and sets paths
- 2) getPNNL14805data() gets all the SPFT data for three glass compositions which are contained in a Excel spreadsheet 'PNNL14805_AppA_SPFT_data.xlsx'. The original data was reported in grams of glass dissolved per unit surface area. This data is back converted to the original moles per unit volume that would have been present in the contacting solution. It also returns information on the glass composition and a list of molecular weights. Only the LAWA44 data is used in further analysis.
- 3) SelectDataSubset(SPFT, irange) selects certain experimental sets as determined by irange and this can be amended by the user. It also eliminates any data that does not contain all four Si, Al, Na and B concentrations.
- 4) calcIAP_aH_wPhreeqc(GlsComp, MW, SPFT, Exp_, nExp) uses Phreeqc and the reported solution concentrations to calculate the ion activity product (IAP) and the hydrogen activity needed in the AH model. It adds these data to the SPFT array but only for experiments in the irange.
- 5) writeParamFiles(par) takes the initial guess at the parameters values (etta, Ea, k and Kgl) and writes these to a file "initialParam.dat" and also makes a copy "estimatedParam.dat" for use by pest.
- 6) firstRun(GlsComp, SPFT, Exp_, nExp, fnPar) runs the model using these initial guesses and writes a file that can be read by PEST and compared to the experimental data.
- 7) writePCFinputFile() writes a file containing the experimental data in the same format as the firstRun file output above but this file becomes part of the larger PEST Control File (PCF).
- 8) initCheckPestFiles(FileNameXLSX, SheetNameXLSX, nPar, nObs) uses a series of templates to prepare the PCF. It uses an Excel file 'PCF/PCF_Input_All_AH.xlsx' to input needed values. The rather cumbersome PEST setup routine is avoided and automated by this process. The routine runs PEST routines that check for a correct file format.
- 9) initHandShaking() ensure that certain signal files created by MatLab and PEST are not present.
- 10) runPestModel(fnPar, SPFT, Exp_, nExp, GlsComp) starts PEST in the background using getML.exe to get the model results. getML.exe does not actually start the model but loops until a signal file is created by MatLab

denoting that new model results are available. After starting PEST, the MatLab routine then falls into a continuous loop that looks for a signal file from PEST indicating that new parameter values are available. It then executes the AH model and writes a new data estimate file. The process continues until PEST determines the best parameter estimate has been reached and ceased to write a new parameter estimate file. If MatLab determines that no new parameter file is present after a suitably long time, $\sim 10X$ that required to solve the model, it also terminates and reports the results in the data structure AH.

- 11) Plot_AH(GlsComp,AH,SPFT, nExp, Exp_) then creates four plots of the data and the AH with the best parameter estimate for four different temperatures.

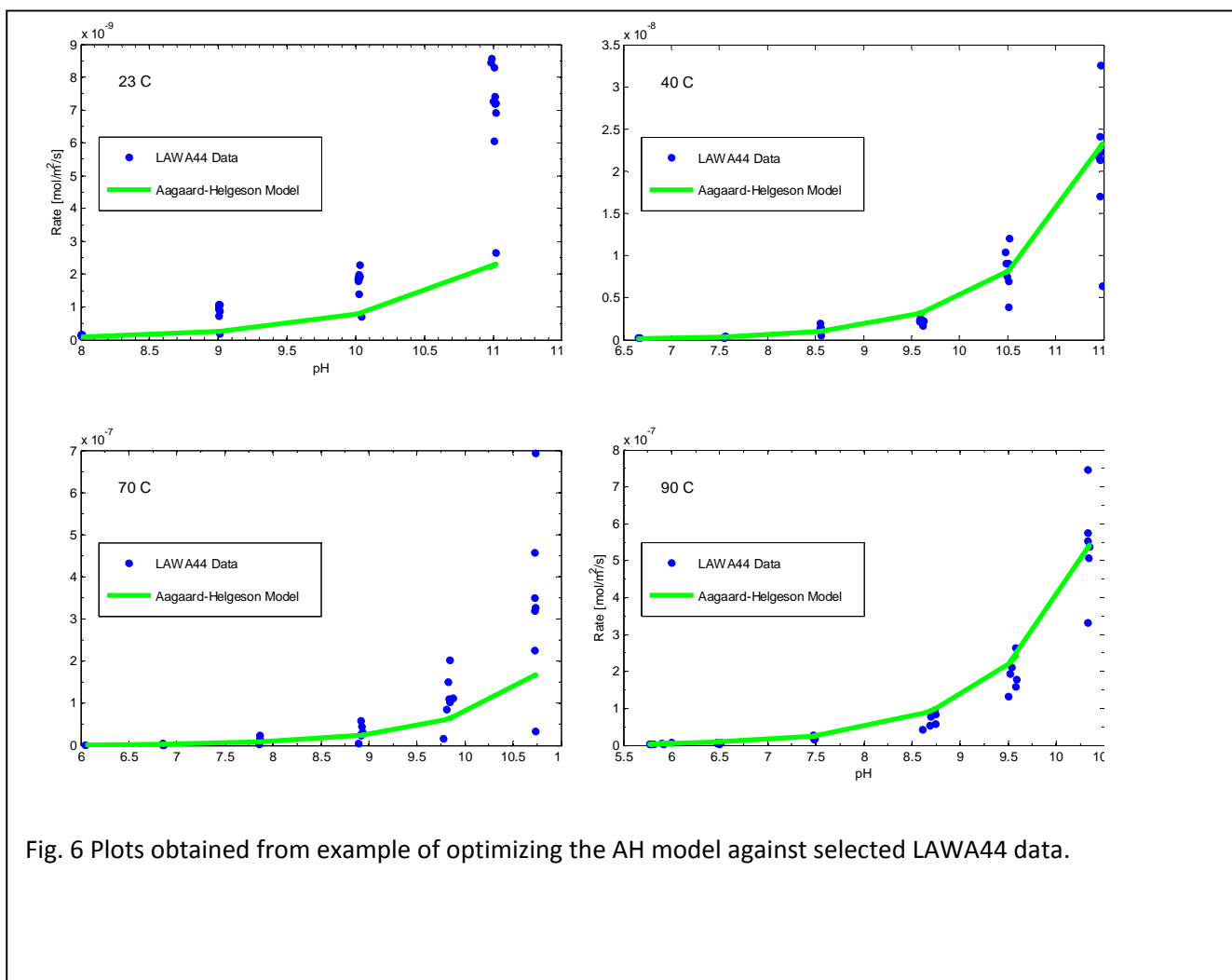


Fig. 6 Plots obtained from example of optimizing the AH model against selected LAW A44 data.

The plots are reproduced in Figure 6 for easy comparison

```
%% Initialize MatLab and Paths
clear all; close all;
Initialize()
```

```

%% Import data from 'PNNL14805_AppA_SPFT_data.xlsx'
[GlsComp, MW, SPFT] = getPNNL14805data();

%% Select data subset for analysis, write to 'selectedMeas.dat'
irange = [08 39 51 45 ...
          09 40 52 46 ...
          12 41 53 47 ...
          14 42 54 48 ...
          16 43 55 49 ...
          44 56 50];
[Exp_ nExp] =SelectDataSubset(SPFT,irange);

%% Phreeqc Calc. of IAP and a_H for each data set in irange
[SPFT] = calcIAP_aH_wPhreeqc(GlsComp, MW, SPFT, Exp_, nExp);

%% Write 'inititalParam.dat' 'estimatedParam.dat' 'PCF/PCF_Param_Data.input'
'PCF/PCF_Param_Gps.input'
% 'inititalParam.dat' is copied to 'estimatedParam.dat' initial for use by PEST.
clearvars par; % prevents inadvertently adding anything to this later on ??
par.etta = 0.5; % H+ power coefficient
par.Ea = 60.0*1e3; % kJ/mol -> J/mol
par.k = 1.3e4/(MW.LAWA44*24*3600); % g/m2/d -> mol of glass/m2/s
par.Kgls = 5.45e-4*1e3; % glass equil coef, mol/L -> mmol/kgw

[fnPar, nPar] = writeParamFiles(par);

%% 1st model run on 'estimatedParam.dat' output to 'initialModelOutput.dat' and copied to
'estimatedModelOutput.dat'
[nObs] = firstRun(GlsComp, SPFT, Exp_, nExp, fnPar);

%% Write 'PCF/PCF_Obs_Data_Synth.input'
writePCFinputFile()

%% Initialize Pest Files
FileNameXLSX = 'PCF/PCF_Input_All_AH.xlsx';
SheetNameXLSX = 'PCF_Input';
initCheckPestFiles(FileNameXLSX, SheetNameXLSX, nPar, nObs)
clearvars FileNameXLSX SheetNameXLSX
fclose('all');

%% initialize Handshaking loop
initHandShaking()

%% Start Pest with getML.exe
[AH] = runPestModel(fnPar, SPFT, Exp_, nExp, GlsComp);

%% Plot the results by Temperature and pH
close all;
Plot_AH(GlsComp,AH,SPFT, nExp, Exp_);

```

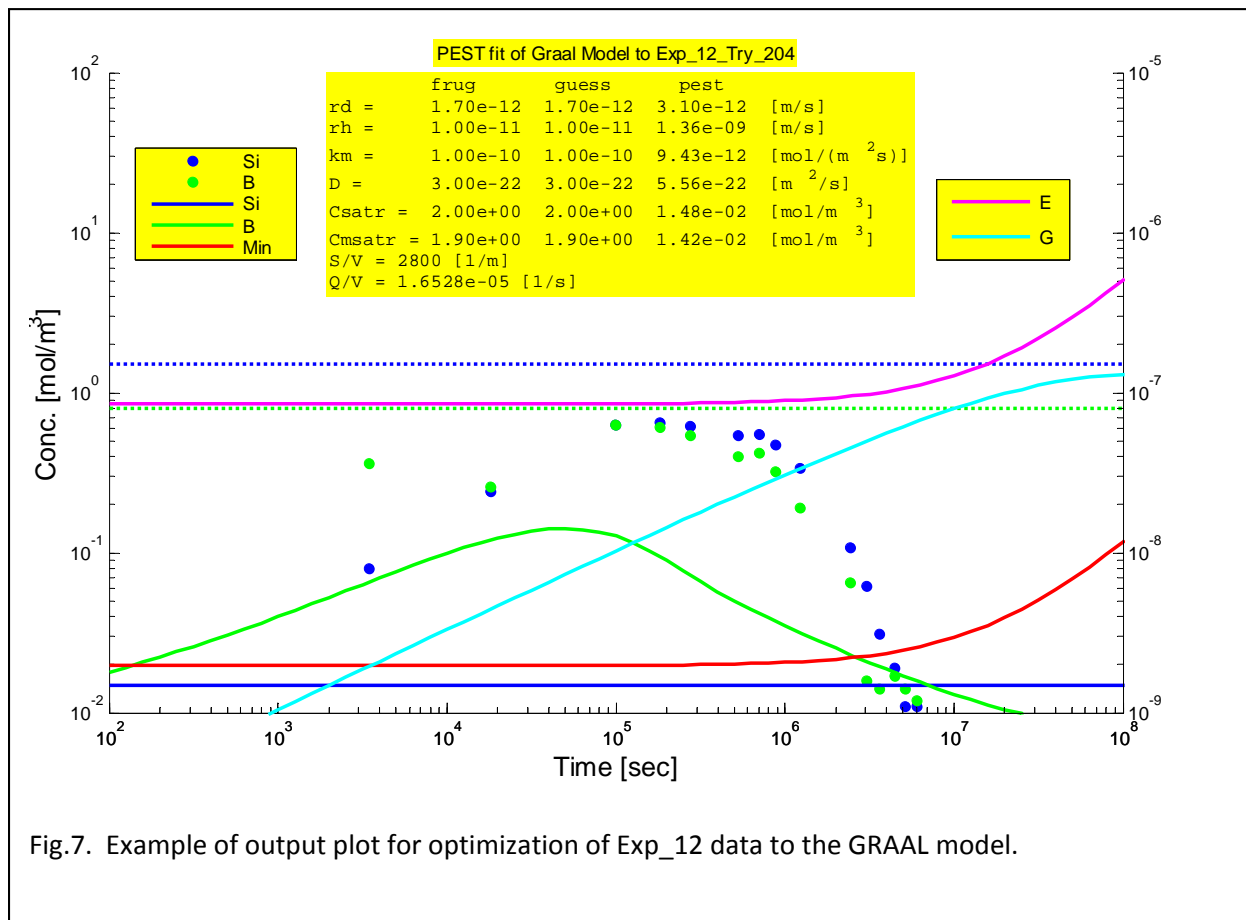
Example2. Optimizing the GRAAL Model against Time Dependent SON68 Data

Example 2 illustrates how the GCMT can be used with time dependent data and a model run via the COMSOL PDE solver. The MainDriver.m file listed below outlines the general procedure. It is similar to that of Example 1 but is more complex because of the call to COMSOL. IPhreeqc is not used in this example but has been used in other cases involving COMSOL. To run this example the entire code should be obtained from the author and will require MatLab, COMSOL with the MatLab LiveLink, and PEST.

The steps are as follows:

- 1) Initialize MatLab by clearing the workspace, deleting unneeded files and adding paths
- 2) User supplies the name of the particular Frugier data set by, for example, names.Exp = 'Exp_12' and providing a "Try" number. The Try number uniquely identifies a particular run and has no other significance. Import_Frugier_Data_V4() as the name suggest imports of all 12 of the SON68 experimental datasets.
- 3) Next the initial guess for the model parameters (rd, rh, km, D, Csatr, Cmsatr, S_V, Q_V, Csi_gls, Cb_gls) are given. In this case the values provided by Frugier are used and modified by multiplication by the vectors synthVec and guessVec using initParam()
- 4) The initial values for the GRAAL variables (C0si, C0b, C0m, E0, G0) are supplied. These are usually set to zero for a pristine piece of glass.
- 5) Then one can choose to make and fit synthetic data. Noise is added to the data. This process is primarily used to test assumptions about the model and observe the result behavior. It can also be used to test the fitting process. If makeSynthData = false then experimental data is analyzed.
- 6) Main_V136() then runs the PEST GRAAL optimization process.
 - a. First a series of empty data arrays are created
 - b. The model is then run with the initial guess of the parameters to create a results file that PEST can compare to the experimental values. The process here for extracting data from COMSOL still works but COMSOL now provides better methods.
 - c. initPestFiles_V3() creates the PCF needed by PEST
 - d. The handshaking loop in then initialized
 - e. Pest is started in the background and the MatLab wait loop is initiated.
 - f. Steps c, d, e. are identical to that in Example 1 except for minor variations.
- 7) The data are then plotted and the workspace and figures saved.
- 8) The final piece of code allows the user to reload a data set and plot a figure.

An example of the plot prepared by the code is given in Figure 7. Note that the GRAAL model does not do a particularly



good job of reproducing the experimental data. Some experiments provide better fits. However a detailed discussion is beyond the scope of this User's Manual.

```

%% MainDriver.m
% This is the top most program which imports Frugier data from an excel
% file and may as desired create synthetic data using the nominal parameters
% as listed by Minet et al. It then initiates the Pest fitting routine and
% finally plots the data. param.synthVec and param.guessVec allow the
% basic Minet parameters to be scaled for creation of synthetic data or
% changing the initial guess of the parameters used by Pest. Some hand
% editing is required to select between analysis of the Frugier data or
% synthetic data.

% called routines
% Import_Frugier_Data_V4
% paramFrug
% initParam
% initVariables
% MakeSynth_Data_V134
%   Graal_CMP_NoNorm_V130(...)
%   mphsolinfo(...)
%   mphgetu(...)

```



```

% Main_V136
%   DeletePestFiles()
%   initSpeciesArrays_V2(...)
%   Graal_CMP_NoNorm_V130(...)
%   mphsolinfo(...)
%   mphgetu(...)
%   initPestFiles_V3(...)
%       PCF_Script_V2(...)
%   Graal_evalModel_V2(...)
% plotGraalPestFit_V2()

%

%% Initialize
close all; clear all;
DeletePestFiles();
addpath('VTTB_VS_Solns');

%% Import Frugier Files
% names.aTry is a unique identifier used to identify a particular run.
% Change this each time a new experimental or synthetic data set is run
% with a particular set of model parameter guesses. names.Exp is the
% Frugier data set selected for analysis

names.aTry=204;
Exp_ID = {'Exp_01';'Exp_02';'Exp_03';'Exp_04';'Exp_05';'Exp_06'; ...
          'Exp_07';'Exp_08';'Exp_09';'Exp_10';'Exp_11';'Exp_12'};
names.Exp = 'Exp_12';

names.HomeDir = pwd;
% Import all Frugier Data and Get data for selected experiment.
[FrugierData] = Import_Frugier_Data_V4([names.HomeDir, '\AllDissDataFrugierJNM2009.xlsx'],Exp_ID);
aFrugExp = FrugierData.(names.Exp);
clear('Exp_ID');
% Experiment sets consist of t, nt, pH, h, si, b, S_V, Q_V, Csi_gls, Cb_gls
% and a few others

%% Setup parameters and initial variables
% Fixes a set of parameter to values reported by Frugier/Minet
% parameter sets consist of:
%   rd, rh, km, D, Csatr, Cmsatr, S_V, Q_V, Csi_gls, Cb_gls
param.frug = paramFrug();
PF = param.frug; % An abbreviation to neaten function calls.

% param.synth and param.guess are obtained by multiplying param.frug by the
% synthVec and guesVec values respectively in the function intiParam. Edit
% or uncomment as desired.

%
%   rd  rh  km  D  Ccatr Cmsatr
param.synthVec = [1.0, 1.0, 1.0, 1.0, 1.0, 1.0];
param.synth = initParam(PF, param.synthVec, PF.S_V, PF.Q_V, PF.Csi_gls, PF.Cb_gls);

% %
%   rd  rh  km  D  Csatr Cmsatr
% param.guessVec = [1.0, 1.0, 1.0, 1.0, 0.1, 10.0];
% param.guess = initParam(param.frug, param.guessVec, PF.S_V, PF.Q_V, PF.Csi_gls, PF.Cb_gls);
% %
%   rd  rh  km  D  Ccatr Cmsatr
param.guessVec = [1.0, 1.0, 1.0, 1.0, 1.0, 1.0];
param.guess = initParam(PF, param.guessVec, aFrugExp.S_V, aFrugExp.Q_V, aFrugExp.Csi_gls,
aFrugExp.Cb_gls);
% Note: select one of param.guess depending upon data to be fit by pest.

param.pest = param.guess;

%% Initialize variables (not parameters) used in COMSOL GRAAL model
initVars = initVariables();

```


Example3. GUI for the ALTGLASS database

Carol Jensen of Savannah River National Laboratory has compiled an extensive database, ALTGLASS, covering many glass leaching experiments usually of the SPFT type. The database is not yet officially released but a copy can be obtained by contacting Dr. Jensen directly. Most of the data in ALTGLASS is not time dependent but 3 or 4 times are reported for a few samples. Unfortunately this is probably not sufficient for parameter optimization with the GRAAL model and the AH and GM with or without consideration of a residual rate is probably the best choice for fitting to this database.

ALTGLASS contains a wealth of information on each experimental point including the glass oxide composition, the leachate concentration, temperature, flow rate, pH etc. Some 68 values are reported for each for the nearly 2000 experiments. This makes it very difficult to parse through the database and find similar experiments or identify possible trends. In addition the ALTGLASS database would provide a useful input the GCMT provided there was a convenient way to select desired data.

Towards this end a graphical user interface for ALTGLASS was constructed using MatLab. Most of the code is obscure in that it relates to creation of interactive windows and not with analysis of data and we won't discuss the details here. A copy of the code can be obtained from the author.

1. Start the code by running Main.m
2. A browser window will pop-up. Browse to the ALTGLASS database and open it
3. After a few seconds to load the database, a table of the entire database will appear as well as a window with four buttons across the top. These are:
 - a. Add Column Selection
 - b. Update Selected Data Table
 - c. Hide/Show Columns
 - d. Plot Data
4. Below these appears a selection box entitled "Select a column from drop down menu" with an initial value of "None" in the drop down menu. The supplied menu represents the columns of data in ALTGLASS. Select a desired category. Depending upon whether the column contain text or numerical values a new interface will appear
 - a. For text values such as "Glass ID", a text entry box will appear as well as a drop down menu. Either type in a value in the text entry box or select a value from the drop down menu. Once a text value is selected it will appear in the text box and may be edited. Usually one will want to shorten the text to include a series of similar data.

- b. For numerical data such as “pH” two sliders will appear representing the minimum and maximum limits that can be selected. These can be adjusted in the conventional manner or specific values entered into the text box.
5. Clicking the “Add Column Selection” button will add up to four selection criteria.
6. Clicking the “Update Selected Data Table” button will create and/or update a table containing only the rows in the database matching the criteria. The criteria can be modified and then the table updated.
7. Hide/Show Columns provide a series of tick boxes that allow one to select which columns are shown in the Selected Data Table. Click the “Update Selected Data Table” after closing the window in view the changes.
8. After making the desired selection, the Boron concentration can be plotted versus time by clicking “Next Step Plot Data” button. Since Boron is often taken as a primary indicator of the degree of glass leaching it provides a rough manner to visualize glass alteration.
9. A model selection box will appear but this is not currently working. This is intended to be the interface to the GCMT as illustrated in other examples.

References

1. Åagaard, P. and H.C. Helgeson, *Thermodynamic and Kinetic Constraints on Reaction Rates among Minerals and Aqueous Solutions. I. Theoretical Considerations*. American Journal of Science, 1982. **282**: p. 237-285.
2. Gin, S., et al., *Theoretical consideration on the application of the Aagaard–Helgeson rate law to the dissolution of silicate minerals and glasses*. Chemical Geology, 2008. **255**(1–2): p. 14-24.
3. Helgeson, H.C., W.M. Murphy, and P. Aagaard, *Thermodynamic and Kinetic Constraints on Reaction Rates Among Minerals and Aqueous Solutions. II. Rate Constants, Effective Surface Area, and the Hydrolysis of Feldspar*. Geochimica et Cosmochimica Acta, 1984. **48**: p. 2405-2432.
4. Grambow, B., *Nuclear Waste Glass Dissolution: Mechanism, Model, and Application*. 1986, Hahn-Meitner-Institut: Berlin, Germany.
5. Grambow, B., *Geochemical modeling of the reaction between glass and aqueous solution*, in *Advances in Ceramics*, G.G. Wicks and W.A. Ross, Editors. 1984, American Ceramic Society: Westerville, OH. p. 474-481.
6. Grambow, B., *A general rate equation for nuclear waste glass corrosion*. Materials Research Society Symposium Proceedings, 1985. **44**: p. 16-27.
7. Grambow, B., *Nuclear waste glass dissolution: Mechanism, model and application*. 1987, JSS Project, Swedish Nuclear Fuel and Waste Management Co. p. 114.
8. Grambow, B., *Modelling approaches: Glass dissolution, Spent fuel dissolution*. 2005.
9. Van Iseghem, P., et al., *GLAMOR. A critical evaluation of the dissolution mechanisms of high level waste glasses in conditions of relevance for geological disposal. Progress report 2001-11-01 to 2003-01-31*. 2003, SCK CEN: Mol, Belgium.
10. Frugier, P., et al., *Application of the GRAAL model to leaching experiments with SON68 nuclear glass in initially pure water*. Journal of Nuclear Materials, 2009. **392**(3): p. 552-567.
11. Frugier, P., et al., *SON68 nuclear glass dissolution kinetics: Current state of knowledge and basis of the new GRAAL model*. Journal of Nuclear Materials, 2008. **380**(1–3): p. 8-21.
12. Minet, Y., et al., *Analytic implementation of the GRAAL model: Application to a R7T7-type glass package in a geological disposal environment*. Journal of Nuclear Materials, 2010. **404**(3): p. 178-202.
13. Jantzen, C., *Altglass Database*, P.c. Rieke, Editor. 2013.

14. Bacon, D.H. and B.P. McGrail, *Waste Form Release Calculations for the 2005 Integrated Disposal Facility Performance Assessment*. 2005.
15. Pierce, E.M., et al., *Waste Form Release Data Package for the 2005 Integrated Disposal Facility Performance Assessment*. 2004, Pacific Northwest National Laboratory: Richland, WA.
16. Wilson, M.L., et al., *Total-system performance assessment for the Yucca Mountain Site*. Materials Research Society Symposium Proceedings, 2002. **713**: p. 153-164.
17. Gin, S., et al., *Contribution of atom-probe tomography to a better understanding of glass alteration mechanisms: Application to a nuclear glass specimen altered 25 years in a granitic environment*. Chemical Geology, 2013. **349–350**(0): p. 99-109.
18. Dell, W.J., P.J. Bray, and S.Z. Xiao, *11B NMR studies and structural modeling of Na₂O · B₂O₃ · SiO₂ glasses of high soda content*. Journal of Non-Crystalline Solids, 1983. **58**(1): p. 1-16.
19. Du, L.-S. and J.F. Stebbins, *Nature of Silicon–Boron Mixing in Sodium Borosilicate Glasses: A High-Resolution 11B and 17O NMR Study*. The Journal of Physical Chemistry B, 2003. **107**(37): p. 10063-10076.
20. Du, L.-S. and J.F. Stebbins, *Site Preference and Si/B Mixing in Mixed-Alkali Borosilicate Glasses: A High-Resolution 11B and 17O NMR Study*. Chemistry of Materials, 2003. **15**(20): p. 3913-3921.
21. Du, L.-S. and J.F. Stebbins, *Network connectivity in aluminoborosilicate glasses: A high-resolution 11B, 27Al and 17O NMR study*. Journal of Non-Crystalline Solids, 2005. **351**(43–45): p. 3508-3520.
22. Dupree, R., et al., *The structure of soda-silica glasses: a MAS NMR study*. Journal of Non-Crystalline Solids, 1984. **68**: p. 399.
23. Zhong, J. and P.J. Bray, *NMR study of structure of sodium boroaluminate glass at high sodium content*. Journal of Non-Crystalline Solids, 1986. **84**(1–3): p. 17-25.
24. Zhong, J. and P.J. Bray, *Change in boron coordination in alkali borate glasses, and mixed alkali effects, as elucidated by NMR*. Journal of Non-Crystalline Solids, 1989. **111**(1): p. 67-76.
25. Davis, K.M. and M. Tomozawa, *Water diffusion into silica glass: Structural changes in silica glass and their effect on water solubility and diffusivity*. Journal of Non-Crystalline Solids, 1995. **185**(3): p. 203-220.
26. Tomozawa, H. and M. Tomozawa, *Diffusion of water into a borosilicate glass*. Journal of Non-Crystalline Solids, 1989. **109**(2–3): p. 311-317.
27. Tomozawa, M., *Water in glass*. Journal of Non-Crystalline Solids, 1985. **73**(1–3): p. 197-204.
28. Tomozawa, M., *Concentration Dependence of the Diffusion Coefficient of Water in SiO₂ Glass*. J. Am. Ceram. Soc., 1985. **68**: p. C-251 - C-252.
29. Tomozawa, M. and K.M. Davis, *Time dependent diffusion coefficient of water into silica glass at low temperatures*. Materials Science and Engineering: A, 1999. **272**(1): p. 114-119.
30. Zhang, Y. and H. Behrens, *H₂O diffusion in silicate glasses and melts*, in *Goldschmidt Conference*. 1998: Toulouse.
31. Zhang, Y., E.M. Stolper, and G.J. Wasserburg, *Diffusion of a multi-species component and its role in oxygen and water transport in silicates*. Earth and Planetary Science Letters, 1991. **103**(1–4): p. 228-240.
32. Zhang, Y.X., *H₂O in rhyolitic glasses and melts: Measurement, speciation, solubility, and diffusion*. Reviews of Geophysics, 1999. **37**(4): p. 493-516.
33. Zhang, Y.X. and H. Behrens, *H₂O diffusion in rhyolitic melts and glasses*. Chemical Geology, 2000. **169**(1-2): p. 243-262.
34. Zhang, Y.X., E.M. Stolper, and G.J. Wasserburg, *Diffusion of Water in Rhyolitic Glasses*. Geochimica Et Cosmochimica Acta, 1991. **55**(2): p. 441-456.
35. Gin, S., et al., *Nuclear Glass Durability: New Insight into Alteration Layer Properties*. J. Phys. Chem. C, 2011. **115**: p. 18696-18706.
36. Cailleateau, C., et al., *Insight into silicate-glass corrosion mechanisms*. Nature Materials, 2008. **7**(12): p. 978-983.
37. Vernaz, E., et al., *Present understanding of R7T7 glass alteration kinetics and their impact on long-term behavior modeling*. Journal of Nuclear Materials, 2001. **298**(Compendex): p. 27-36.
38. Van Iseghem, P., et al., *GLAMOR: A Critical Evaluation of The Dissolution Mechanisms of High Level Waste Glasses in Conditions of Relevance for Geological Disposal*. 2007.

39. Ryan, J.V., et al., *Towards Improved Models for Waste Glass Corrosion*. 2009: Pacific Northwest National Laboratory.
40. Bird, B.R., W.E. Stewart, and E.N. Lightfoot, *Transport Phenomena*. 2nd ed. 2002, New York: John Wiley & Sons, Inc.
41. Crank, J., *The Mathematics of Diffusion*. Second Edition ed. 1975, Oxford: Clarendon Press.
42. Carslaw, H.S. and J.C. Jaeger, *Conduction of Heat in Solids*. 2nd ed. 1959: Oxford Science Publications.
43. Krishna, R. and J.A. Wesselingh, *The Maxwell-Stefan approach to mass transfer*. Chemical Engineering Science, 1997. **53**(6): p. 861-911.
44. Wesselingh, J.A. and R. Krishna, *Mass Transfer in Multicomponent Mixtures*. 2000: Delft University Press.
45. Marshall, W.L. and E.U. Franck, *Ion Product of Water Substance, 0-1000 C, 1-10,000 Bars, New International Formulation and its Background*. J. Phys. Chem. Ref. Data, 1981. **10**(2): p. 295-304.
46. Aagaard, P. and H.C. Helgeson, *Thermodynamic and kinetic constraints on reaction rates among minerals and aqueous solutions I. Theoretical considerations*. American Journal of Science, 1982. **282**: p. 237-285.
47. Grambow, B. and R. Müller, *First-order dissolution rate law and the role of surface layers in glass performance assessment*. Journal of Nuclear Materials, 2001. **298**(1-2): p. 112-124.
48. Eyring, H., *The Activated Complex in Chemical Reactions*. J. Chem. Phys, 1935. **3**: p. 107.
49. Laidler, K.J. and M.C. King, *Development of transition-state theory*. The Journal of Physical Chemistry, 1983. **87**(15): p. 2657-2664.
50. Gin, S., et al., *Theoretical consideration on the application of the Aagaard-Helgeson rate law to the dissolution of silicate minerals and glasses*. Chemical Geology, 2008. **255**(1-2): p. 14-24.
51. Pierce, E.M., et al., *An experimental study of the dissolution rates of simulated aluminoborosilicate waste glasses as a function of pH and temperature under dilute conditions*. Applied Geochemistry, 2008. **23**(9): p. 2559-2573.